DISSERTATIONES
PHYSICAE
UNIVERSITATIS
TARTUENSIS
148

ANDREI GORONOVSKI

Systematic study and NORM-LCA methodology development of NORM aspects in the bauxite residue valorization chain

DISSERTATIONES PHYSICAE UNIVERSITATIS TARTUENSIS
148

DISSERTATIONES PHYSICAE UNIVERSITATIS TARTUENSIS
148

ANDREI GORONOVSKI

Systematic study and NORM-LCA methodology development of NORM aspects in the bauxite residue valorization chain

UNIVERSITY OF TARTU
Press
1632

This study was carried out at the Institute of Physics, Faculty of Science and Technology, University of Tartu, Estonia.

The dissertation was admitted on 13.05.2026 in partial fulfilment of the requirements for the degree of Doctor of Philosophy in Physics and was allowed for defense by the Council of the Institute of Physics, University of Tartu.

Supervisor: Associate Professor Alan Henry Tkaczyk,
Faculty of Science and Technology,
University of Tartu, Estonia

Opponent: Professor Wouter Schroeyers,
Faculty of Engineering Technology,
Hasselt University, Belgium

Defense: 02.09.2026 at the University of Tartu

The research leading to these results has received funding from the European Union's Horizon 2020 research and innovation programme (H2020/2014–2019) under Grant Agreement No. 636876 (MSCA-ETN REDMUD). This publication reflects only the authors' view, exempting the European Union from any liability. The author would like to acknowledge the support of an STSM Grant from COST Action TU1301 NORM4Building, supported by the COST Association (European Cooperation in Science and Technology).

cost
EUROPEAN COOPERATION
IN SCIENCE & TECHNOLOGY

Funded by the Horizon 2020
Framework Programme of the
European Union

ISSN 1406-0647 (print)
ISBN 978-9908-57-235-2 (print)
ISSN 2806-2523 (pdf)
ISBN 978-9908-57-236-9 (pdf)

University of Tartu Press
www.tyk.ee

ABSTRACT

This thesis presents a comprehensive study of the Naturally Occurring Radioactive Materials (NORM), namely ^{238}U, ^{234}Th and ^{40}K in the bauxite residue (BR) valorization chain, incorporating a NORM impact category within the international Life Cycle Assessment (LCA) methodology. The research addressed the potential environmental and health concerns associated with radiological impacts arising from metallurgic residue valorization. Two primary goals were achieved during this work: (1) development and implementation of NORM impact category within LCA methodology and (2) characterization of BR valorization streams from a radiological perspective.

A new integral model was developed to cover the gaps considering NORM within LCA based on the set of state-of-the-art modeling tools and internationally recognized radiological conversion factors. Radiological assessment of the BR valorization streams was performed using gamma-ray spectroscopy.

It was demonstrated that the newly developed NORM-LCA impact category covered considerable risks to human health that have been historically overlooked in the methodology. Particularly, it was demonstrated that radiological impact from natural radionuclides present in the living premises resulted in the highest damage to people compared to existing LCA impact categories. It was also demonstrated that impact from incorporating BR into construction materials would be minor compared to existing impacts.

During radiological characterization of the Bayer process dissolution of ^{40}K and minor portion of ^{238}U was observed. It was confirmed that minor content of natural isotope ^{238}U ended up in the alumina reaching concentration of 5 Bq/kg, while the rest radionuclides were not detected in alumina and ended up in the BR.

It was demonstrated that multi-stage valorization processes of BR can be achieved without significant radionuclide accumulation in the secondary residues. It was confirmed that radioactivity concentrations in the materials resulting from BR valorization would be too low to pose a health threat from the radiological standpoint. It was observed that equilibrium decay chains of natural uranium and thorium can be broken during chemical and metallurgical treatment of BR, with isotopes from a single chain ending up in different streams. A future study is suggested to analyze radionuclides recovered with valuable metals, and connect the solubility and co-recovery of radionuclides with mineral phases they exist in.

ABSTRACT IN ESTONIAN

Süstemaatiline uuring looduslike radioaktiivsete ainete (NORM) aspektidest boksiidijääkide väärtusahelas ja NORM-olelusringi analüüsi metoodika arendamine

See dissertatsioon esitab põhjaliku uuringu looduslikult esinevate radioaktiivsete materjalide (NORM), nimelt ^{238}U, ^{234}Th ja ^{40}K kohta boksiidijääkide (BR) ümbertöötlemise ahelas, lisades NORM-mõjukategooria rahvusvahelise olelusringi analüüsi (LCA) metoodikasse. Uuring käsitleb jääkide ümbertöötlemist tulenevate radioloogiliste mõjudega seotud võimalikke keskkonna- ja tervisemõjusid. Selle töö käigus saavutati kaks peamist eesmärki: (1) NORM-mõjukategooria lisamine LCA metoodikasse ja (2) BR-ümbertöötlemise protsesside iseloomustamine radioloogilisest vaatenurgast.

Loodud uus integraalmudel NORM-i arvestamiseks LCA-s kasutades tipptasemel olemasolevaid modelleerimisvahendeid ja rahvusvaheliselt aktsepteeritud iseloomustustegureid. BR-ümbertöötlemise protsesside radioloogiline hindamine viidi läbi gammakiirguse spektroskoopia abil.

Näidati, et äsja väljatöötatud NORM-LCA mõjukategooria hõlmas märkimisväärseid mõjusid inimeste tervisele, mida metoodikas on ajalooliselt tähelepanuta jäetud. Eelkõige näidati, et ehitatud keskkonnas esinevate looduslike radionukliidide radioloogiline mõju põhjustas inimestele suurimat kahju võrreldes olemasolevate LCA mõjukategooriatega. Samuti näidati, et BR-i lisamise mõju ehitusmaterjalidesse oleks olemasolevate materjalidega võrreldes väike.

Bayeri protsessi radioloogilise iseloomustamise käigus täheldati ^{40}K ja väikese osa ^{238}U lahustumist töötlemislahustites. Kinnitati, et väike osa looduslikust isotoopist ^{238}U jõudis alumiiniumoksiidi, saavutades kontsentratsiooni 5 Bq/kg, samas kui ülejäänud radionukliide alumiiniumoksiidis ei tuvastatud.

Näidati, et BR-i mitmeastmelisi ümbertöötlemise ahelaid saab saavutada ilma olulise radionukliidide akumuleerumiseta sekundaarsetes jääkides. Kinnitati, et BR-i ümbertöötlemise protsessidest tulenevad radioaktiivsuse kontsentratsioonid materjalides on radioloogilisest seisukohast liiga madalad, et kujutada endast terviseohtu inimestele. Täheldati, et loodusliku uraani ja tooriumi tasakaalu lagunemisahelad võivad BR-i keemilise ja metallurgilike töötlemise käigus katkeda, kusjuures ühe ahela isotoobid jõuavad erinevatesse toodetesse. Soovitatakse tulevikus läbi viia uuring, milles analüüsitakse väärtuslike metallidega eraldatud radionukliide ning seostatakse radionukliidide lahustuvust ja kaaseraldamist mineraalfaasidega, milles nad esinevad.

TABLE OF CONTENTS

LIST OF PUBLICATIONS

The current thesis is based on the following publications. These publications are referred to with corresponding Roman numbers throughout the text.

I. P. J. Joyce, **A. Goronovski**, A. H. Tkaczyk, and A. Björklund, "A framework for including enhanced exposure to naturally occurring radioactive materials (NORM) in LCA," *Int. J. Life Cycle Assess.*, vol. 22, no. 7, 2017. https://doi.org/10.1007/s11367-016-1218-2

II. **A. Goronovski**, P. J. Joyce, A. Björklund, G. Finnveden, and A. H. Tkaczyk, "Impact assessment of enhanced exposure from Naturally Occurring Radioactive Materials (NORM) within LCA," *J. Clean. Prod.*, 2017. https://doi.org/10.1016/j.jclepro.2017.11.131

III. P. J. Joyce, T. Hertel, **A. Goronovski**, A. H. Tkaczyk, Y. Pontikes, and A. Björklund, "Identifying hotspots of environmental impact in the development of novel inorganic polymer paving blocks from bauxite residue," *Resour. Conserv. Recycl.*, vol. 138, no. April, pp. 87–98, 2018. https://doi.org/10.1016/j.resconrec.2018.07.006

IV. **A. Goronovski**, J. Vind, V. Vassiliadou, D. Panias, and A. H. Tkaczyk, "Radiological assessment of the Bayer process," *Miner. Eng.*, vol. 137, no. April, pp. 250–258, 2019. https://doi.org/10.1016/j.mineng.2019.04.016

V. **A. Goronovski** and A. H. Tkaczyk, "Radiological assessment of the bauxite residue valorization chain," *J. Radioanal. Nucl. Chem.*, vol. 321, no. 3, pp. 955–963, 2019. http://doi.org/10.1007/s10967-019-06676-6

VI. **A. Goronovski**, R. M. Rivera, T. Van Gerven, and A. H. Tkaczyk, "Radiological assessment of bauxite residue processing to enable zero-waste valorisation and regulatory compliance," *J. Clean. Prod.*, vol. 294, p. 125165, 2021. http://dx.doi.org/10.1016/j.jclepro.2020.125165

AUTHOR CONTRIBUTION TO PUBLICATIONS

I. Andrei Goronovski was equal contributor to the literature review, model selection and description. Andrei Goronovski participated in the development of the final framework and was responsible for writing significant number of sections of the manuscript. Peter James Joyce was the main contributing author. Alan Henry Tkaczyk and Anna Björklund provided support and supervision.

II. Andrei Goronovski was a joint first author of this article with Peter James Joyce. The work on the model, writing manuscript and results analysis was split in half between Andrei Goronovski and Peter James Joyce. Case study was performed mainly by Peter James Joyce. Alan Henry Tkaczyk, Göran Finnveden and Anna Björklund provided support and supervision.

III. Andrei Goronovski prepared and analyzed samples for the radionuclide concentrations, developed infrastructural module for the NORM-LCA model and wrote corresponding chapter. The rest of the research and manuscript writing was performed by Tobias Hertel and Peter James Joyce. Alan Henry Tkaczyk, Yiannis Pontikes and Anna Björklund provided support and supervision.

IV. Andrei Goronovski prepared samples and performed measurements. Results analysis and mass-flow calculations were performed with the help of Johannes Vind. Andrei Goronovski was the main author of the manuscript, while Johannes Vind contributed by writing chapter 1 and performed mass-flow calculations, reviewed and supported all the other chapters. Vicky Vassiliadou, Dimitrios Panias and Alan Henry Tkaczyk provided support and supervision.

V. Andrei Goronovski prepared samples, performed measurements, analyzed results and wrote manuscript under support and supervision of Alan Henry Tkaczyk.

VI. Andrei Goronovski prepared samples and performed measurements. Results analyses were performed with the help of Rodolfo Marin Rivera. Andrei Goronovski was the main author of the manuscript, while Rodolfo Marin Rivera contributed by writing an explanation of the chemical processes used to produce samples and participated in the result analysis. All the figures were prepared by Rodolfo Marin Rivera. Tom Van Gerwen and Alan Henry Tkaczyk provided support and supervision.

LIST OF ABBREVATIONS

ACI – activity concentration index
AR – accumulation ratio
BR – bauxite residue
DALY – disability adjusted life years
DCC – dose conversion coefficient
EF – exposure factor
EU BSS – European basic safety standard
ILCD – The International Reference Life Cycle Data System
LCA – life cycle assessment
NORM – naturally occurring radioactive material
OPC – ordinary Portland cement
PAF – potentially affected fraction
PDF – potentially disappeared fraction
REE – rare-earth elements

1. INTRODUCTION

Over 95% of the worldwide primary aluminum production is accounted to the Bayer process [1]. Bauxites, aluminum bearing ores are dissolved in a strong sodium hydroxide caustic solution to form aluminum hydroxide, which later is converted to alumina (aluminum oxide, Al_2O_3). All the remaining elements of the bauxite, mostly insoluble, are filtered and accumulated in the residue. This byproduct is called bauxite residue (BR) or red mud and nowadays it is mostly stored in landfill sites. On average, 1.35 tons of BR is produced per 1 ton of alumina, and after conversion to the metal form, this corresponds to roughly 3 tons of BR per one ton of primary aluminum [2].

Considerable efforts have been made to find industrial application for this material [1], for instance in the form of construction applications, landfilling or residue mining. However, these efforts so far had limited success as up today, less than 3% of the annually produced bauxite residue is valorized [3]. Considering that the demand for aluminum is constantly growing, and therefore quantities of produced residue (mass of worldwide bauxite residue (BR) production has increased roughly by 50% during 2010–2019, [4]), a more comprehensive solution is needed to tackle this issue.

The European Union's Horizon 2020 research and innovation programme (Grant Agreement no. 636876) MSCA-ETN REDMUD project aimed to provide such a solution by developing zero-waste bauxite residue method that would allow to extract the valuable metals and incorporate remaining secondary residues in the construction materials. This was planned to be achieved by developing multi-step valorization chains of the bauxite residue. For instance, by recovering major component of the BR – iron, remaining elements would further be enriched and could be extracted more efficiently. Valorization of the industrial waste streams would have direct benefits in the form of reduced landfill sites, new workplaces, conservation of natural resources, increased economic security through production of critical raw metals, etc. However, some of the potential benefits would not be that evident, or even arguable. For instance, reduced environmental damage due to utilization of the waste streams or potential reduction of emissions. One might argue that the separation of metals from bauxite residue would be a more energy consuming process than conventional extraction process and therefore would result in bigger environmental damage.

Another potential negative effect of residue valorization is the accumulation of minor hazardous elements (toxic or radioactive) or release of these elements to the environment. One might need to answer the question: "Would it be safer for the environment and society to keep bauxite residue in the landfill sites or to utilize it?" Concerning bauxites, these contain trace amounts of toxic elements, such as chromium, arsenic, lead, and natural radionuclides present in most of the ores in quantities that are not harmful. Extraction of aluminum from bauxites results in the accumulation of these trace elements in the residue. Further extraction of valuable metals from the bauxite residue might lead to potential release of these

elements to the environment or to further increase of these minor elements in the secondary residues to the point that they would pose a hazard. It is important to determine how these elements behave during processing and what would be their impact on humans and the environment.

In order to characterize benefits and drawbacks arising from a novel process and to compare it with traditional technologies or alternative processes, a comprehensive method is required that would assess all the impacts of the process from the cradle to the grave. This method would also need to compare different types of impacts, e.g. reduction of landfill areas versus increased energy consumption. Life Cycle Assessment (LCA) is an internationally recognized methodology which would allow us to compare processes' impact on the environment and humanity in a variety of impact categories. LCA is a systematic methodology to assess environmental impacts of products, processes or services from cradle to the grave. For a specific product this would include raw material extraction and transportation, manufacturing, product utilization and disposal or recycling at the end of life. However, LCA lacks a methodological basis to assess the influence of natural radionuclides and thus should be improved. This can be done by developing a new impact category within LCA that would cover all potential impacts coming from natural radionuclides.

In order to facilitate valorization of the bauxite residue, this research thesis focuses on the natural radionuclides presented in the bauxite residue and sets two goals: (a) to incorporate Naturally Occurring Radioactive Materials (NORM) impact category within life cycle assessment methodology and (b) to characterize bauxite residue valorization streams from a radiological perspective.

2. THEORETICAL BACKGROUND

2.1. Bayer process description

Current study is performed in the association with Mytilineos S.A. aluminum plant, which utilizes Bayer process to produce aluminum. Plant's feed inventory is comprised of roughly 80% karst bauxite [5] coming from Greece and Turkey and 20% lateritic (also known as tropical) bauxite [6] from Ghana or Brazil.

The Greek bauxite initially goes through the decalcitation stage to remove excess of limestone. Limestone contains organic matter that would have negative effects during bauxite dissolution stage. This processing stage is specific for the current plant due the nature of the bauxites mined in Greece. Then bauxites from Greece and Turkey are mixed and go through the grinding and crushing stage. Lateritic bauxite is also grinded and crushed, however it goes on a separate conveyor and is mixed with spent sodium hydroxide solution coming from the alumina precipitator, whereas karst bauxite is mixed with a concentrated sodium hydroxide solution. Calcium oxide is added to the karst bauxite slurry to improve efficiency of the alumina digestion [7]. Digestion of karst bauxite takes place first, and the lateritic bauxite slurry is added at a later stage to improve process productivity. Prior to mixing, lateritic bauxite slurry remains in a desilication container, where silica reacts with aluminum to form sodium aluminum silicate, which precipitates and would eventually end up in the bauxite residue. See **Figure 1** for more details.

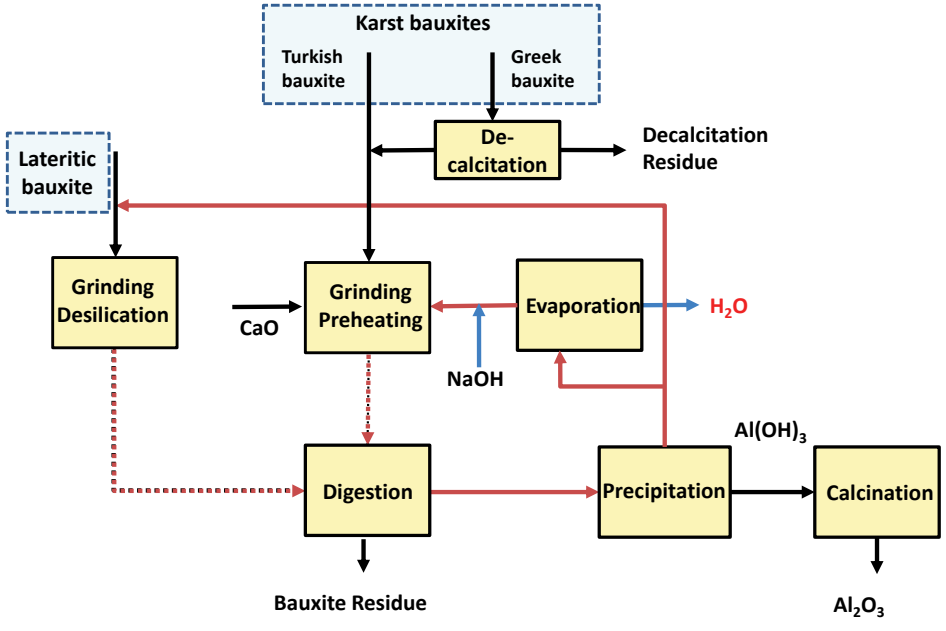

Figure 1: Bayer process at Mytilineos S.A. aluminum plant.

Next, separation of insoluble impurities happens during settling stage. Separated material is a slurry with high water content and can be named red mud. Mytilineos S.A. plant utilizes filter press to dewater residue. Water is reused at the plant, and the resulting bauxite residue is landfilled. Precipitation and calcination of alumina are performed conventionally [8], [9].

2.2. Bauxite residue

Historically, residue from the Bayer process was produced in the form of slurry with high moisture content and was considered a waste material and was called red mud. It was often discharged into sea or stored into specific residue disposal areas [10]. Advances in environmental protection awareness have led to abandoning of the sea discharge methods. A pooling method gained popularity next, which resulted in construction of large ponds or areas surrounded by dams, where red mud was dumped. The growing volume of the produced bauxite residue requires production of new disposal areas and puts an economic burden on the alumina plants. Subsequently, multiple failures of the residue disposal areas (Ajka accident in Hungary in 2010 [11], Mariana dam disaster in Brazil in 2015 [12] or Dahegou accident in China in 2016 [13]) have demonstrated that this stockpiling method is potentially dangerous to nearby population and can be highly hazardous for the environment. As a result, adding filter press stage to the aluminum plants is becoming popular. Residue slurry is dewatered and turned into low moisture solid material. Such material can be classified as bauxite residue, to distinguish it from high moisture slurry, often referred to as red mud. Bauxite residue can be easily stored in landfill sites.

2.3. NORM in bauxite residue. Accumulation, issues

Most of the ores and rock in the Earth crust contain trace quantities of natural radionuclides, the most common of these are ^{238}U, ^{232}Th and ^{40}K, as well as decay products of the first two. These isotopes are often called primordial, as they have been presented in the Earth crust since its creation and have half-lives comparable with the lifetime of the universe. These are present in the soil, construction materials, our bodies or even food products. Nevertheless, these radionuclides can pose similar radiological hazard if accumulated to high ratios as the artificial ones produced during nuclear fuel cycle. The accumulation is the process of the concentration of radionuclides during chemical or mechanical processing of materials. Examples of natural radionuclide accumulation can cover wide ranges of essential industrial processes: water purification, cement production, burning of coil, mineral ore separation, etc.

European Basic Safety Standard (EU BSS) sets 1 mSv effective dose as the limit for public exposure from all man-made practices for all EU member states [14]. For comparison, the dose that an average member of the public is getting

from the environment equals 2.4 mSv according to the UNSCEAR [15], but this value strongly varies worldwide. These doses remain far below doses that can cause any harm to a person. For instance, the lowest known does attributed to increased risk of having cancer is 100 mSv [16].

In order to avoid complex assessment of every industry dealing with raw materials, a screening limit is recommended by EU BSS [14] to disregard materials that are unlikely to cause elevated radiological exposure. For natural radionuclides these are summarized in **Table 1**. Once these limits are exceeded by a material used in an industry, this does not necessarily imply that it would be dangerous to workers or the public, but that a further assessment might be needed to guarantee public and worker safety. In general, the processing of natural resources is often associated with dangerous chemicals (ex. acids, alkalis), high temperatures, hazardous particulate matter etc. Considerable worker safety measures are required, and these are usually superficial regarding natural radionuclides.

Table 1: Radionuclide concentration ranges for bauxite residues worldwide and specific concentrations for Mytilineos S.A. plant. Measurement uncertainties are reported at the confidence level of 2σ.

Radionuclide	Worldwide concentration [Bq/kg][17]	Mytilineos S.A. plant mean concentration [Bq/kg]	EU BSS screening limit [Bq/kg] [17]
^{238}U	10–9000	170 ± 2	1000
^{228}Ra (^{232}Th)	35–1400	431 ± 7	1000
^{228}Th (^{232}Th)	35–1400	404 ± 15	1000
^{40}K	10–600	26 ± 8	10 000

BRs from around the world (see **Table 1**) have high variability of radionuclide concentrations and some can be challenging to process and handle from a radiological perspective. For the BR coming from Greece the EURATOM screening limits are not exceeded and therefore this material does not pose any health hazard from radiological perspective. However, iron oxide comprises roughly 50% of the Greek BR and complete recovery of this compound alone could potentially double radionuclide content in the potential secondary residue, thus elevating potential hazards. Therefore, current study gives a closer look from radionuclide accumulation perspective at the processes developed to valorize BR.

2.4. Bauxite residue processing

Bauxite residue represents a wide range of chemically different materials with their properties summarized in the **Table 2**. High variability in chemical composition is explained by the properties and origin of aluminum bearing ore, as well as differences in the technological processes. In the current study the focus was on the specific bauxite residue coming from the Mytilineos S.A. plant in Agios Nikolaos, Greece.

Table 2: Chemical composition of currently studied bauxite residue and typical composition ranges.

Component	Mytilineos S.A. [wt.%] [18]	Typical composition [wt.%] [2]
Fe_2O_3	46.7	5–60
Al_2O_3	18.1	5–30
SiO_2	7.3	3–50
TiO_2	5.8	0.3–15
CaO	8.5	2–14
Na_2O	2.8	1–10

It can be noticed that BR is rich in valuable minerals and therefore can be further processed. Additionally, some specific BRs can be rich in rare-earth elements (REE), which content in BR is often enriched compared to the bauxite ore and can be further increased by recovery of primary metals (Fe, Al, Ti). For the specific BR, total REE content has been reported around 1000 ppm [19], with main contributors: La, Ce, Nd. The scandium content was 128 ppm [20], which is of high interest due to its highest economic value.

Review of different BR valorization options is discussed elsewhere [21], however, the general conclusion is that single stage processing (i.e. recovery of a specific component) is often inferior economically when compared to conventional resource production methods. For instance, efficient recovery of iron, the most abundant component of BR, has been successfully demonstrated on a pilot scale [22] for the Greek BR. Pig iron has been efficiently recovered using reduction smelting and the resulting slag was turned into mineral wool fiber without any wastes, however, upscaling to a full commercial operation never happened due to economic reasons.

Therefore, the aim of the REDMUD project is to develop a multistage valorization process, where every subsequent processing stage would be enhanced by the prior stage. For instance, recovery of iron can produce secondary residue that would have enriched ratios of aluminum, titanium and REE compared to the initial BR and thus be more of an interesting candidate for further processing. Example of such idealized process is presented in **Figure 2**, where after multiple stages of valorization the final residue would be utilized as construction material establishing zero waste process chain. The figure provides idealized process, as the residue volume would not necessarily decrease at every stage, as every processing stage is associated with addition of excess chemicals, be it fluxing materials, catalysts, or solutions/acids.

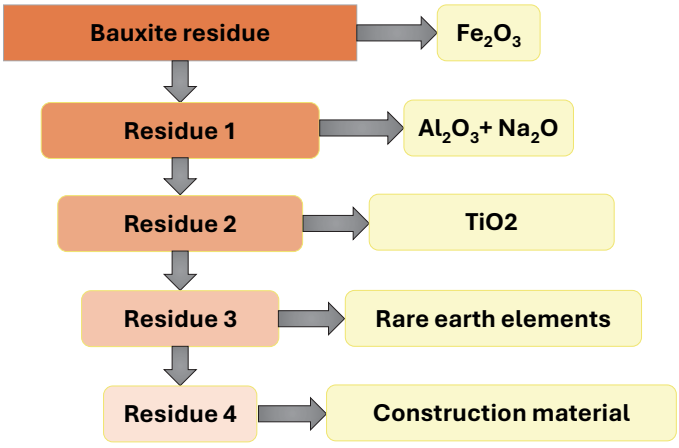

Figure 2: Idealized zero waste BR processing chain.

The idealized process flowsheet demonstrates multistage valorization path. However, in reality each stage of the processing may have additional input materials (like limestone in the reduction roasting process) and sometimes radionuclides can be diluted in the newly produced residue or even recovered altogether with the valorized metals. Better understanding of the radionuclides' behavior during processing would help optimize processes considering radiological impacts. Overall, the radionuclide change in the secondary residues (accumulation ratio, *AR*) is presented in the form of the activity concentration in the secondary residue over the activity concentration in the BR as in equation 1. In case of a multistage process the ratio over initial BR is presented.

$$AR = \frac{C_{new\ residue}}{C_{BR}} \quad (1)$$

2.5. Discussion of the bauxite residue processing methods

The reduction-based smelting of iron

An electric arc furnace was employed for the reclamation of pig iron from the BR, where carbon (coal) was utilized to transform iron oxides into metallic iron at elevated temperatures, ranging from about 1500 to 1700 °C [23]. Consequently, the iron was reclaimed in the form of pig iron (crude iron with high carbon content, produced by smelting industries), while the remaining materials were separated as slag. This is a widely used method for iron production from iron ore.

To enhance the separation between pig iron and slag, additional fluxing materials such as lime and SiO_2 could be introduced into the process. A minor amount of flue dust was generated as an extra secondary waste product, which holds the potential for recycling by other industries [24], [25].

Reduction roasting of iron

Iron roasting served as an alternative technique for reclaiming iron from BR by converting the iron within BR into a magnetic state [26]. In this process, BR was blended with metallurgical coke, and sodium carbonate (Na_2CO_3) was incorporated as a fluxing agent. The resulting mixture underwent roasting at a temperature of 1000 °C, resulting in the formation of cinders (sodium aluminates). These cinders were subsequently subjected to milling and leaching with water. The resulting particles were then subjected to multiple rounds of magnetic separation. Different levels of electrical currents were applied to the magnet. Consequently, a significant portion of the iron was recovered in the form of magnetic fractions, while the remaining constituents were identified in the non-magnetic fraction (secondary residue), which was then analyzed for radionuclides. It has been reported that > 99% of iron can be converted to magnetic phases by such approach [26].

Alkali leaching of alumina

In a manner akin to iron roasting, alkali leaching was the process used to combine BR with sodium carbonate at temperatures between 800–1100 °C to produce cinders [21]. Subsequently, cinders were dissolved in sodium hydroxide (NaOH). Next, they were recovered, leaving the remaining substances as a residue. Sodium aluminate cinders are subsequently processed to recover alumina.

Acidic metal recovery

First, BR was neutralized with CO_2 to lower its pH, consequently minimizing acid consumption, as outlined elsewhere [18]. Next, mineral acids (H_2SO_4, HNO_3, HCl) were applied to dissolve both primary and trace metals present in the BR. Radionuclide concentration of the resulting solid residue was then measured.

Ionic liquid leaching

Ionic liquids are characterized by their ability to melt at low temperatures (<1000 °C), they melt without decomposing and exist in a molten state composed solely of ions. Thus, ionic liquids exhibit potent solvent properties and are an alternative to mineral acids for dissolving BR and extracting various metals, including REE. In the current project, a specific ionic liquid, namely 1-Ethyl-3-Methylimidazolium Hydrogen Sulphate (abbreviated as [Emim] [HSO_4]), was employed to leach valuable metals from BR. The selection of this specific ionic liquid was based on its proven high recovery rate for scandium [27], element providing significant economic incentive for BR valorization. Throughout this process, valuable metals were dissolved, entering the leachate, while the insoluble fractions were filtered and designated as a secondary residue, which were then analyzed for the radionuclides.

2.6. Bauxite residue in construction materials

Bauxite residue is an interesting choice as a construction material constituent. It has both environmental and economic implications. From an environmental perspective utilizing BR in cement industry has two primary benefits: (1) reduction of residue streams and (2) production of low carbon cement to help reach EU net greenhouse gas emissions [28].

Economical motivation for BR valorization in cement industry comes from high aluminum and iron content which are required additives in the cement production [2], [29]. Currently BR utilized in cement industry comprises only up to 3–5% of conventional Portland cement raw mix [1]. Portland cement is currently the most used cement type worldwide. The problem here is that such a low percentage of BR in cement cannot consume all the residue streams, as well as the transportation to the cement plants can be costly. One option to improve situation is to develop novel cement batches that would utilize significantly higher fraction of BR. An example would be the development of iron rich high strength cement with BR content up to 50% [30]. These so-called calcium sulfoaluminate-based cements can achieve similar or better mechanical properties as Portland cement while potentially having significantly lower carbon emissions [30]. These would highly rely on industrial by-products, such as metal slags, fly ashes or bauxite residue that currently have limited or no use at all and are often treated as wastes. Byproducts could partially substitute limestone used in cement clinker manufacturing: limestone is heated in the rotary kiln over temperature of 1350 °C to "burn out" organics and release CO_2 to the environment. By utilizing industrial by-products, the amounts of released CO_2 are greatly reduced, as well as energy required to heat up limestone.

An alternative solution is to produce inorganic polymer materials. These are materials with solid polymeric matrix without carbon atoms. They provide considerable interest from the waste management perspective as they can utilize various metallic slags as an alternative to concrete with similar or even superficial mechanical properties. The production of an inorganic polymer can be simplified as follows: a precursor material (ex. bauxite residue), is mixed with activating solution (ex. potassium or sodium silicate solution in water) to start and form a polymerization reaction and to yield a paste that can be shaped. This paste can be pressed and treated with temperature to form building blocks. In this manner, newly produced materials would utilize BR in bulk amounts (previous research has reported that good compressive strength can be achieved at 85 wt.% BR [31]).

Another option would be to use BR as a filler material (ex. during road construction), also utilizing in bulk amounts. For instance, this idea has already been implemented on practice in Australia [1]. However, in this case additional environmental studies might be needed such as leaching experiments to confirm that all the potentially hazardous elements would be retained in the material.

2.7. LCA

LCA is an internationally recognized and widely used methodology to assess the impact of products or processes along their whole lifecycle on a set of various environmental impact categories, such as ozone layer depletion, global warming, resource depletion, ionizing radiation, etc. it quantifies all relevant resources, emissions and impacts in a comprehensive way. LCA considers product's full life cycle, from resource extraction, to manufacturing, use phase and up to the final disposal or reusing. Methodology principles and framework are described by international standards ISO 14040 and 14044 [32], [33].

LCA can be used to compare the environmental burden of similar products, or to assess environmental impact hotspots of a process during the design phase. In order to assess a product, its inventory, including supply and production chains, must be assessed. Then the concept of midpoint and endpoint factors is utilized, which quantify the impact by the product.

2.8. NORM for LCA

LCA already includes ionizing radiation impact category, however, this only covers artificial radionuclides (nuclides coming from nuclear fuel cycle). The ILCD handbook considers extension of radionuclides covered within the LCA methodology as a high priority task [34]. Particularly, literature overview has demonstrated that naturally occurring radionuclides are mostly overlooked within LCA methods, even though they provide by far major dose of ionizing radiation to public (Publication I). Moreover, the fate of these nuclides and exposure pathways can differ significantly from the artificially produced radionuclides. Therefore, a decision was made to develop a separate LCA impact category, that would specifically address impact from NORM.

3. RESEARCH METHODOLOGY

3.1. LCA

According to the International Reference Life Cycle Data System (ILCD) handbook [35] ISO standard 14040:2006 [33] the key LCA steps are:

1. **Goal and scope definition.** Identifying reasons for the study, defining products or services to be studied, understanding study boundaries and limitations.
2. **Inventory analysis.** Gathering best available data on all inputs and outputs of elementary flows for every stage of the product life cycle.
3. **Impact assessment.** Translating inventory data into environmental impact indicators (ex. climate change, resource depletion, ecotoxicity, etc.). In the current study SimaPro 8 software was used for impact assessment. This step can be subdivided into key parts:
   - 3.1. **Fate assessment** models how the chemicals behave in the environment with the help of fate factors.
   - 3.2. **Exposure assessment** estimates how chemicals come into contact with the recipients.
   - 3.3. **Effect assessment** focuses on the harm that comes from the chemicals released into the environment.
   - 3.4. **Damage assessment** translates effects into actual harm to human population or ecosystem.
4. **Result interpretation.** Analyzing results, answering questions posed during goal definition, assessing uncertainties and accuracy of the results.

In order to justify development of a new impact category for the LCA method, firstly review of existing methods for ionizing radiation was performed. Currently existing models that cover the topic of ionizing radiation, for instance, developed by Meijer [36], [37], Frischknecht [38], Garnier-Laplace [39] were assessed. It was determined that: (1) current LCA tools do not sufficiently cover natural radionuclides, (2) fate and exposure pathways of natural radionuclides can vary significantly from the artificially produced nuclides.

Next, all relevant to NORM release and exposure pathways were identified using the lifecycle of bauxite residue as an example. After that, a literature review has been performed to identify suitable models that could be applied to characterize different stages of the LCA (fate, exposure, damage) for NORM materials in two impact categories: humans and biota. These model candidates were systematically reviewed and assessed along multiple scientific criteria as suggested by the EU Joint Research Centre [40]:

- Completeness of scope: *To which extent are the NORM exposure mechanisms covered for the environment and humans?*
- Model relevance: *How relevant is the model to different stages of the LCA method?*

- Robustness and certainty: *Has the model been validated or peer reviewed? Are the model shortcomings and uncertainties reported?*
- Applicability: *How applicable is the model for NORM materials and the LCA methodology? Can it be applied directly, or does it require modifications?*
- Transparency and reproducibility: *How accessible are the model data and documentation? Can it be reproduced?*
- Stakeholders' acceptance: *Is the model currently used? Is it accepted by the authorities?*

The results of the models' assessment were selection of multiple most suitable ones to cover all the stages of LCA and all the possible release pathways (Publication I). The proposed framework was later implemented to calculate midpoint and end-point factors, using bauxite residue valorization options as a case study. The model was then evaluated and verified against other models (Publication II).

3.2. Radiological assessment

3.2.1. Sample preparation and measurement

In order to recover valuable metals, BR has been subjected to a series of chemical and metallurgical processes. Secondary residue samples have been tested for the radionuclide content with gamma-ray spectroscopy.

All the samples discussed in the current thesis were prepared in a similar manner: solid samples were crushed and grinded to form homogeneous powder like structure, liquid samples were dried under infra-red lamps. And then the resulting dried mass crushed and grinded. Then samples were dried at 105 °C for 24 hours. Finally, samples were sealed based on the available mass:

1. Bulk samples that were coming mostly from industry and that were available in large amounts were tightly packed and sealed in 55.5 cm^3 aluminum containers.
2. Experimental samples that were usually available in the order of 0.5–5 grams were mixed with a larger mass of epoxy resin to form a homogeneous mixture covering bottom of aluminum containers. Then the containers were tightly sealed.

After sealing, samples were kept intact for 30-day period in order for ^{226}Ra and its decay products to reach secular equilibrium [41]. In some specific cases, where ^{234}Th (decay product of ^{238}U) was measured, samples were kept intact for 6 months so that the equilibrium between ^{234}Th and ^{238}U was reached. Measurements have been performed with high purity Germanium detectors: GEM-35200 (EG&G Ortec) coaxial detector and BE3830P (Canberra) broad energy detector. Measurement results were analyzed with GammaVision (Canberra) software.

In order to reduce measurement uncertainty, samples were prepared in the same way as the measurement standards including container geometry, sample

preparation process and sealing method. Potential differences in the density and chemical matrix between sample and standards were corrected using EFFTRAN tool [42]. For the measurement standards, uranium and thorium samples provided by IAEA (RGU-1 and RGTh-1) [43] were used. This allowed for direct measurement of ^{238}U and ^{232}Th decay products using peak to peak calibration technique, thus avoiding unnecessary uncertainties (for instance, potential uncertainty due to radon leakage from the container can reach 6.5% [44]). To measure ^{40}K calibration curve was built using above mentioned standard materials. List of measured radionuclides (with corresponding daughter nuclides and gamma energy lines) are summarized in **Table 3**.

To measure background spectra, the same empty containers as for the samples were used, however measurement time was at least 72 hours.

Table 3: List of gamma energies used in the detection of studied nuclides. In brackets corresponding shorter-lived daughter nuclides that were used for measurement are provided.

Isotope series	Isotope	Gamma line energy [keV]
^{238}U	^{238}U (^{234}Th)	63.3
	^{226}Ra (^{214}Pb)	242.0 295.2 351.9
^{232}Th	^{228}Ra (^{228}Ac)	338.3 911.2 969.0
	^{228}Th (^{212}Pb)	238.6
^{40}K	^{40}K	1460.8

3.2.2. Construction materials

As recommended by the EU BSS, Activity Concentration Index (ACI) is a screening tool that can be applied to assess final construction materials, see equation (2) [14], [45]. These were calculated once the gamma measurements of the construction materials were done. If the value of the index is below one, the construction material poses no potential harm and can be used without any limitations. If the index is between one and six, the material application is limited to superficial and infrastructural applications, ex. tiles, roads, wall coatings, etc. It should be noted, however, that these are recommended screening values: there is a variety of limiting ACIs or even different correlations to calculate this factor in different countries (for instance, in Finland correlation for infrastructural materials includes ^{137}Cs).

$$ACI = \frac{C_{Ra-226}}{300} + \frac{C_{Th-232}}{200} + \frac{C_{K-40}}{3000} \quad (2)$$

4. RESULTS AND DISCUSSION

4.1. Development of NORM-LCA impact assessment method

In order to characterize impact of natural radionuclides, steps described in the **Figure 3** would need to be considered. Determination of the inventory is usually scenario specific. In our case, several theoretical BR valorization scenarios were investigated: (1) 'business as usual', in which BR is conventionally landfilled near the production site, (2) production of pre-fired bricks with BR content up to 30% and (3) 3% BR addition to ordinary Portland cement inventory. The radionuclide content of this residue was measured directly with gamma-spectroscopy as discussed in section 3.2 .

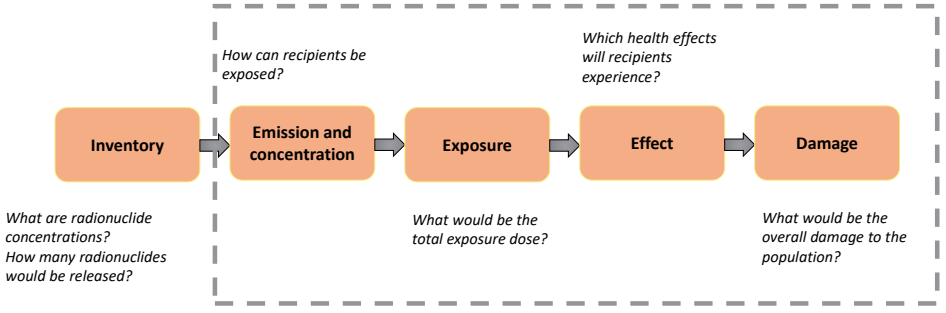

Figure 3: Key steps of the LCA model for natural radionuclides. Steps outlined with the dashed lines are the scope of the current model development.

Next, a literature review has been performed to determine existing state of the art tools that could be used as building blocks in the development of comprehensive LCA model. The models have been assessed based on the list of criteria provided in the section 3.1 and the NORM-LCA framework has been suggested using state of the art knowledge, where available. For the knowledge gaps, missing parameters and characterization factors were derived.

4.1.1. Model for impact on humans

To cover all the potential exposure pathways to humans, model presented in the **Figure 4** has been developed in the following way:

- Fate of the natural radionuclides released to the environment was estimated with the USEtox [46], [47] model. USEtox is LCA model used to assess potential toxicological impacts from chemicals released to the environment. For some of the isotopes, the fate data was missing, however, it was possible to derive using chemical and physical properties of the elements (Publication II).

- For humans, the fate factors were multiplied by exposure factors calculated by the USEtox model. USEtox considers exposure to recipients via inhalation and ingestion routes. The exposure factors were multiplied by the dose conversion coefficients (DCC) provided by the UNSCEAR [48] to estimate cumulative dose for humans. For external exposure by gamma radiation assumption of instantaneous homogeneous mixing was used, which is consistent with the USEtox modeling approach. DCCs for radionuclides presented in soil contaminated to infinite depth from Eckerman and Ryman [49] were used to derive exposure factors (EF), as presented in the equation (3), where V_{soil} is the volume of soil used in the USEtox model (Publication II):

$$EF = \frac{DCC_i}{V_{soil}} \quad (3)$$

- For the radionuclides incorporated into construction materials it was assumed that they are bound and cannot be released to the environment. Therefore, gamma radiation is the only means of exposure, which was estimated by the Meijer et al. model [36], [37] for indoor applications and Joyce et al. (Publication III) provide characterization factors for the outdoor (infrastructural) applications. The assumption that radionuclides are bound to the material where they are incorporated is valid for most of the natural radionuclides, except for radon, which is a noble gas and can easily escape from solid structures.
- Radon surface exhalation model provided by UNSCEAR [15] was used to estimate radon indoor concentration. The same model allows to convert indoor dose to exposure using DCCs. For the outdoor radon exposure, it was estimated that the effect would be negligible due to radon dilution in the air (Publication III).
- To estimate exposure at a workplace, Markkanen storage model [45] was used. Since all the potential radionuclide releases to the environment are already accounted for in the previous modelling steps, occupational exposure here consists only of the onsite gamma exposure due to stored materials, which was covered by the Markkanen storage model.
- To convert cumulative dose into damage, concept of Disability Adjust Life Years (DALY) was used [50], which was introduced by Murray for World health Organization [51]. This concept allows us to convert exposure into number of years lost due to early mortality or disabilities. The conversion factors from [man.Sv] to DALYs were summarized by Frischknecht et. al. [38] based on the epidemiological studies of ionizing radiation.

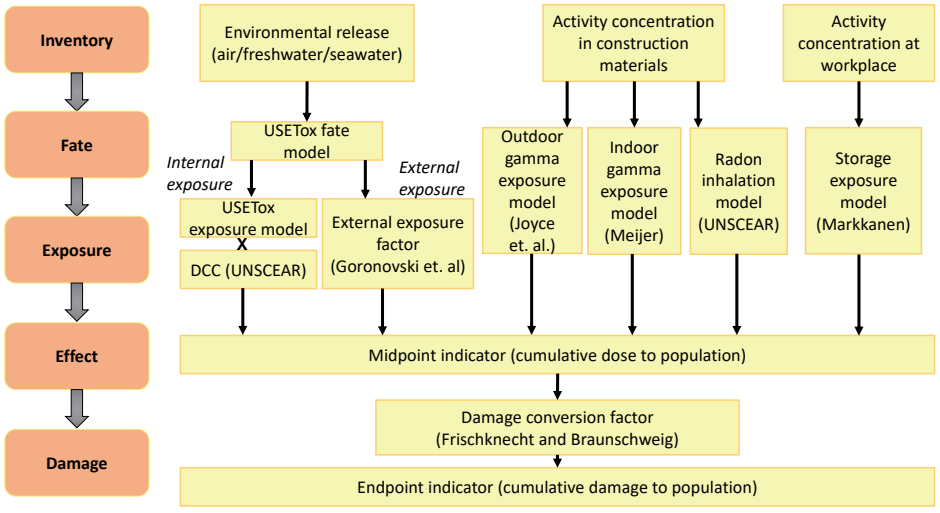

Figure 4: Diagram of the NORM-LCA impact category for humans.

After combining models together as presented in **Figure 4**, mid-point and end-point characterization factors were derived. The model input (inventory) is provided in the radionuclide quantity in the units of Becquerel [Bq]. The collective dose to population (midpoint indicator) is expressed in man Sieverts [man.Sv] and the damage (endpoint indicator) in the DALY. The derived midpoint and endpoint indicators are summarized elsewhere (Publication II) and can be applied directly within existing LCA models.

4.1.2. Model for impact on biota

For the biota, it was assumed that the only possible exposure pathways would be due to environmental release, as wild organisms are mostly unlikely to spend significant amount of time in contact with man-made objects or at industrial sites. This assumption complies with the midpoint and endpoint indicators, which do not focus on individual organisms, but instead on potentially affected fraction of species (PAF) and potentially disappeared fraction (PDF or also called extinction rate) of species respectively. These indicators do not look at a single organism, however, instead rely on possible effects and damage to species and to the ecosystem as a whole. PAF for a single isotope demonstrates a fraction of species adversely affected by this isotope and PDF stands for a fraction of species that could be potentially lost due to the introduction of this isotope to the ecosystem. Selected indicators are consistent with existing LCA methods for other LCA impact categories [52].

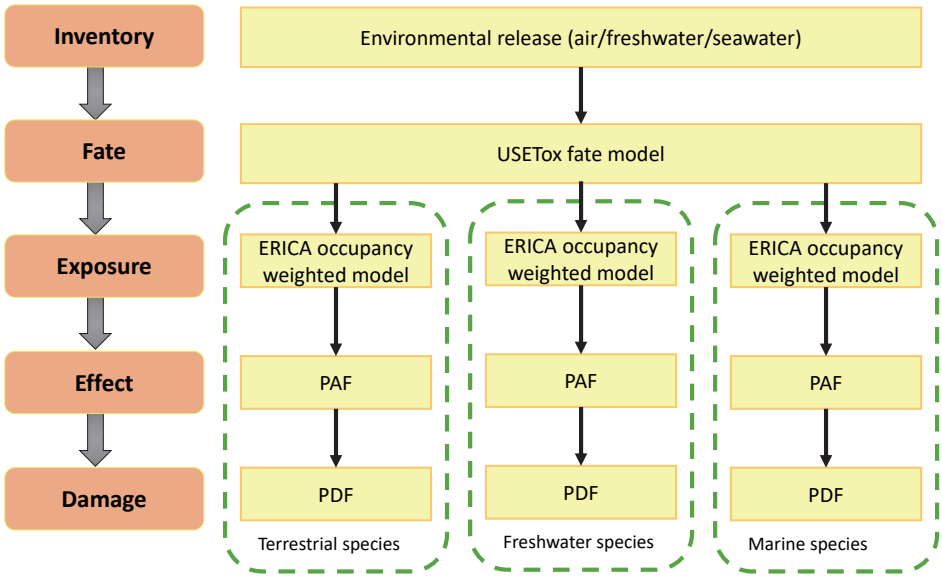

Figure 5: Diagram of the NORM-LCA impact category for biota.

- Combined NORM-LCA environmental model is summarized in **Figure 5**.
- Fate stage of the environmental releases is calculated in the same way as for humans using USETox model. Then 3 separate ecosystems are considered with different representative organisms: terrestrial, marine and freshwater [53].
- The exposure full dose conversion coefficients ($F_{i,o}$) are calculated with the adjusted ERICA model [53] for different groups of species representing typical terrestrial, freshwater and marine organisms using equations (4–6[1]) derived according to Beresford et al. [54]. For terrestrial species equation (4) is used; for freshwater and marine organism equation (4) is used for species living in the water column, (5) is used for organisms living on the sediment and (6) is used for species living in the sediment.

$$F_{i,o} = DCCext_{i,o} + DCCint_{i,o} \cdot CR_{i,o} \quad (4)$$

$$F_{i,o} = 0.5 \cdot DCCext_{i,o} \cdot (1 + Kd) + DCCint_{i,o} \cdot CR_{i,o} \quad (5)$$

$$F_{i,o} = DCCext_{i,o} \cdot Kd_i + DCCint_{i,o} \cdot CR_{i,o} \quad (6)$$

[1] $F_{i,o}$ – full dose conversion coefficient for organism o, caused by isotope i
$DCCext_{i,o}$ – dose conversion coefficient for external exposure
$DCCint_{i,o}$ – dose conversion coefficient for internal exposure (due to ingestion and inhalation)
$CR_{i,o}$ – concentration ratio between environment and organism
Kd_i – concentration ratio between sediment and environment

- As a midpoint indicator, PAF is used as suggested by Garnier-Laplace, et al. [39]. PAF combines both lethal and non-lethal effects on organism groups per unit of radionuclide released. Single factors are provided for every ecosystem considered (terrestrial, freshwater and marine) for every natural radionuclide of interest. In the article by Garnier-Laplace, et al. [39] PAF factors for freshwater ecosystem have been derived and these are used in the current study. For the other two ecosystems PAF factors are derived using equations 7–10:

$$PAF_{e,i} = \frac{0.5 \cdot \Delta C_{e,i}}{HC_{50,e,i}} \tag{7}$$

$$HC_{50,e,i} = \sqrt[n]{EC_{50,e,i,1} \cdot EC_{50,e,i,2} \cdot \ldots \cdot EC_{50,e,i,n}} \tag{8}$$

$$EC_{50,e,i,o} = \frac{HDR_{50,e}}{F_{i,o}} \tag{9}$$

$$HDR_{50,e} = \sqrt[n]{EDR_{10,e,1} \cdot EDR_{10,e,2} \cdot \ldots \cdot EDR_{10,e,n}} \tag{10}$$

- Potentially affected fraction of species for ecosystem *e* and isotope *i* is predicted by equation 7, where $\Delta C_{e,i}$ is the change of the isotope concentration and $HC_{50,e,i}$ is the geometric mean of half maximal effective concentrations $EC_{50,e,i,o}$ for *n* reference organism groups obtained with equation 8. $EC_{50,e,i,o}$ as in the equation 9 is the dose rate related to 10% radiological effect increase for 50% of species over full dose conversion coefficient for a reference organism group *o* caused by isotope *i*. $HDR_{50,e}$ is the geometric mean value of dose rate responses ($EDR_{10,e}$) over a single ecosystem *e* for *n* reference organisms as in the equation 10. EDR_{10} is a chronic dose rate at which the negative effect (mortality, morbidity, reproduction failure) for a reference organism is increased by 10% [55]. The unit for the midpoint indicator is $\Delta PAF \cdot m^3 \cdot d$.
- To estimate damage, conversion coefficient from the USETox model is used as presented in the equation 11 [47] and resulting damage factor is obtained in the units of $\Delta PDF \cdot m^3 \cdot d$ as the endpoint indicator. This indicator demonstrates how the studied process or product will affect the rate of species extinction within the studied ecosystem (freshwater, seawater or terrestrial), focuses on general species biodiversity and not providing any indicators related to single species.

$$PDF = 0.5 \cdot PAF \tag{11}$$

- Most of the modeling parameters (ex. radionuclide transfer coefficients, dose responses and conversion coefficients) are scenario independent and therefore the user of the models needs to know only released radionuclide amounts and pathways to estimate damage to the environment.

4.1.3. NORM-LCA model application

Scenarios description

In order to validate and demonstrate the newly developed model, a case study has been performed considering possibilities of BR valorization withing European Union. Three theoretical scenarios have been selected:

1. Business as usual scenario: the BR is stockpiled in the designated landfill area near the plant.
2. Production of fired bricks with 30% BR addition. The bricks would be used in the production of dwellings.
3. Production of ordinary Portland cement with the addition of 3% BR, also to be used in the construction of dwellings. Ordinary Portland cement composition: 90.25% clinker, 4.75 gypsum, 5% limestone was taken from the Ecoinvent database [56].

The functional unit of the study is the utilization of 1 kg of BR. Due to considerable differences in the scenarios, a concept of 'equal basket of benefits' is used [57], [58]. This is a commonly used technique for waste management analysis: all the scenarios are equivalent with the only difference coming from different fate of BR, meaning that in the first scenario one kilogram of BR is stored in the landfill, while 3.33 kg of bricks and 33.3 kg of Portland cement are produced as normal. In scenarios 2 and 3 one kilogram of BR substitutes corresponding components in the inventory of produced materials and therefore BR is not landfilled. However, after 75 years (mean lifetime of a dwelling), building materials are assumed to be stored in the inert landfills, with no potential radionuclide release to the environment [59]. This assumption differs significantly for the one used for the BR landfilling area; however, it comes from the Ecoinvent database, which assumes that hazardous elements are efficiently immobilized within the construction materials.

Inventory analysis

The Ecoinvent 3.2 database [60] is used as the data source for the inventory analysis and description of the original processes. For the bricks produced with BR, we assume that 30% of the wet clay mass is replaced with residue prior to firing. It has been previously demonstrated [61] that with such ratio mechanical properties of bricks are not altered. For the Portland cement 3% of the clinker material is replaced with BR, and the resulting material would have comparable mechanical properties to the original cement [62].

The radiological properties of the ordinary materials have been taken from the EU database prepared by Trevisi et al. [63]. BR coming from Mytilineos S.A. plant has been discussed in the **Table 1**. As both bricks and cement were assumed to be used in the dwellings, radon exhalation to the living premises must be considered. Radon flux from the construction material to the dwelling is described

by equations 12 and 13 [48], where C_{Ra} stands for ^{226}Ra concentration (radon precursor), λ is the decay constant of the corresponding isotope, f and ρ are the emanation fraction and density of the specific material, d is the material half thickness, L is the diffusion length of material and D_e and is the material specific diffusion length

$$J_D = C_{Ra} \cdot \lambda_{Ra} \cdot f \cdot \rho \cdot L \cdot tanh(\frac{d}{L}) \quad (12)$$

$$L = \sqrt{\frac{D_e}{\lambda_{Rn}}} \quad (13)$$

The following parameters were assumed: radon emanation fraction from concrete (f) = 0.2 [45], from bricks = 0.0035 [64]. Radon diffusion length (D_e) in concrete = $3.0 \cdot 10^{-8}$ ($m^2 \cdot s^{-1}$) and for bricks = $1.9 \cdot 10^{-7}$ ($m^2 \cdot s^{-1}$) [65]. The rate of radon entry into the dwelling (U) is obtained using equation 14, where S_B is the sum of surface areas and V is the dwelling volume [48]. The equation 15 for the excess of the radon concentration (C) [Bq·m^{-3}] in the dwelling air is then derived based on Markkanen study [45], where n is the house ventilation rate.

$$U = 3.6 \cdot 10^3 \cdot S_B \cdot \frac{J_D}{V} \quad (14)$$

$$C = \frac{U}{n} \quad (15)$$

Results: human impact

Results for the human impact for three proposed scenarios are summarized in the **Figure 6** (considering midpoint indicators) and **Table 4** (endpoint effect). BR use phase indicates damage coming from the application of construction materials where BR was incorporated. The overall damage to humans is rather similar in all the scenarios, with the minor increase in scenarios 2 and 3, where BR is used as an additive to construction materials. The main portion of impact comes from the conventional construction materials, which can incorporate a certain quantity of natural radionuclides. The impact from the construction materials to human health is 3 to 4 orders of magnitude higher than the impact from the other exposure pathways. The exposure that is coming from releases to the environment or remaining processes does not only include BR as a source of natural radionuclides but also accounts for previously overlooked natural radionuclides that come from different industries. An example of these industries would be cement production, which results in the environmental release of ^{210}Pb (a long-lived daughter radionuclide of ^{238}U), or releases of ^{210}Pb and ^{210}Po (daughter radionuclides of ^{238}U) from the coal-fired power plants. These releases are already accounted for in the LCA databases such as Ecoinvent [59], [66], however radiological impacts have not been characterized prior to the current study.

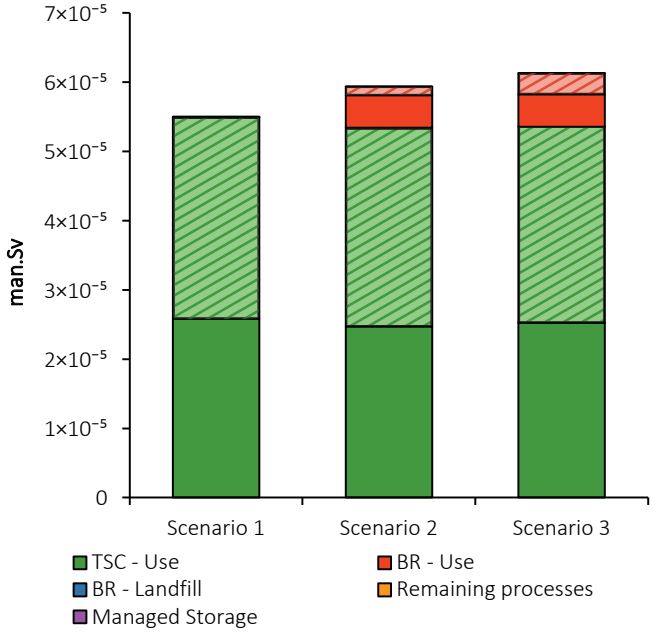

Figure 6: Processes contributing to NORM exposure in humans. TSC: Traditional Supply Chain. Solid bar: gamma dose, hatched bar: radon dose (reprinted from [67]).

Table 4: Processes contributing to the NORM impact category for humans during BR valorization process.

Process	Scenario 1 [DALY]	Scenario 2 [DALY]	Scenario 3 [DALY]
Release to the environment	$2.3 \cdot 10^{-8}$	$4.2 \cdot 10^{-9}$	$4.2 \cdot 10^{-9}$
BR in construction materials (gamma exposure)	0	$7.1 \cdot 10^{-6}$	$7.1 \cdot 10^{-6}$
BR in construction materials (radon exposure)	0	$1.9 \cdot 10^{-6}$	$4.6 \cdot 10^{-6}$
Conventional construction materials (gamma exposure)	$3.9 \cdot 10^{-5}$	$4.4 \cdot 10^{-5}$	$4.5 \cdot 10^{-5}$
Conventional construction materials (radon exposure)	$4.4 \cdot 10^{-5}$	$4.5 \cdot 10^{-5}$	$4.7 \cdot 10^{-5}$
Managed Storage	$1.7 \cdot 10^{-8}$	0	0
Remaining processes	$6.4 \cdot 10^{-9}$	$6.4 \cdot 10^{-9}$	$6.4 \cdot 10^{-9}$
TOTAL	$\mathbf{8.3 \cdot 10^{-5}}$	$\mathbf{9.0 \cdot 10^{-5}}$	$\mathbf{9.3 \cdot 10^{-5}}$

The addition of BR to construction materials exhibits for human exposure an acceptable increase, which is a minor effect compared to impacts from conventional construction materials. It is observed that BR incorporated in concrete has a lower impact than BR incorporated in bricks, due to radon exhalation rates.

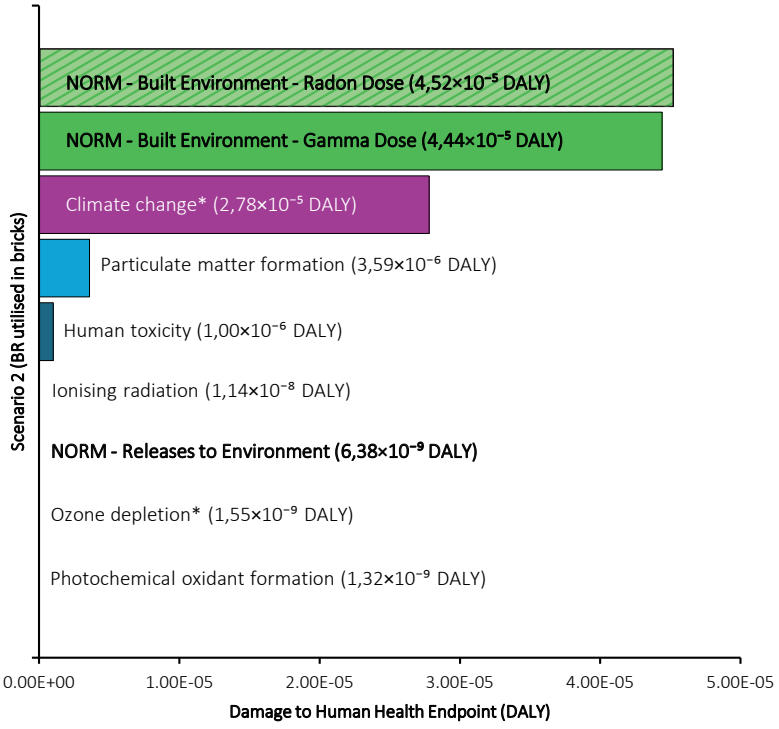

Figure 7: Comparison of damage to human health coming from different LCA impact categories for scenario 2. Results presented in bold are attributed to the newly developed NORM characterization model. Results denoted with '*' correspond to the interim methods according to ILCD [68]. Reprinted from [67].

A cross comparison of the NORM impact category with other existing within LCA impact categories for human health is presented in the Figure 7 for scenario 2, where BR was utilized in the production of firing bricks. Newly characterized impact categories demonstrate dominating risks to human health in comparison with the existing ones, while only damage from climate change is of the same magnitude. As it was already discussed, NORM exposure coming from construction materials is similar for all three investigated scenarios. Radiological exposure is a consideration for both conventional and novel construction materials, as some existing construction materials already may contain some quantity of natural radionuclides. The BR materials considered in this study were found to exhibit only minor radiological characteristics.

The formation of particulate matter and toxicity of the released elements are two other considerable impacts, however, their damage to health is order of magnitude lower compared to damage from NORM in built environments. Damage from NORM released to the environment is similar to the one coming from the ionizing radiation.

Ionizing radiation is an existing impact category within LCA that accounts only for the nuclear fuel cycle and radionuclides that are produced artificially.

The appearance of the damage caused by artificial radionuclides is explained by the energy inventory – the European energy market was used as a data source for the case study, where nuclear power is present at a considerable scale.

Results: environmental impact

The damage to different ecosystems is summarized in the **Figure 8**. The trend is similar to every ecosystem – incorporation of BR in the construction material would have favorable effect on the damage that this residual material impacts on the biota, reducing potentially disappearing fraction of species roughly 80 times for freshwater species, 2 times for marine organisms and 1.5 times for terrestrial. Please keep in mind that these numbers have a more qualitative nature derived in a similar manner to the other environmental impact categories presented in LCA, whereas human impact category provides quantitative results that can be converted for instance to excess cancer cases or early mortality cases.

Results for the environmental damage are highly driven by the long-term emissions from the BR landfilling sites to the groundwaters (see Publication II for further discussion). This is specifically explained by the assumptions used. In case BR is utilized in construction materials, it was assumed that the final fate of these materials would be an inert landfill from which no releases occur, which is in accordance with the guidelines suggested by the Ecoinvent database, version 3 [59].

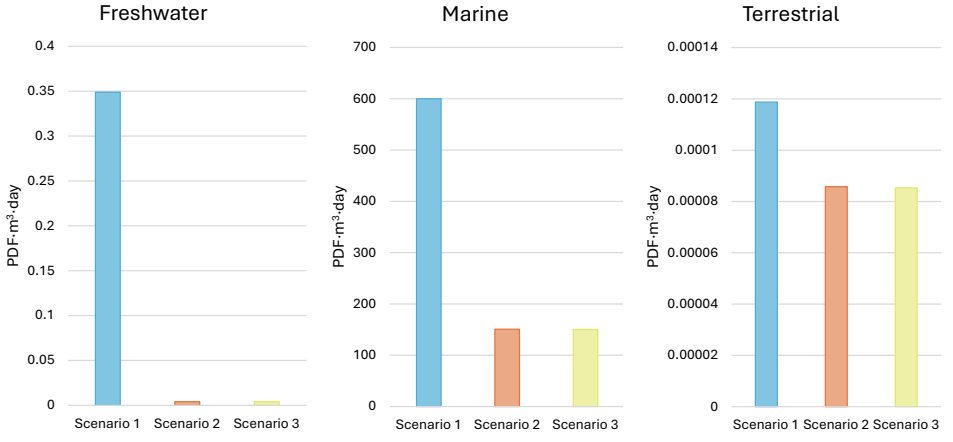

Figure 8: Endpoint results for environmental damage considering three different ecosystems.

For environmental damage current factors cannot be directly compared with the existing factors from other LCA impact categories as different method for the factor derivation was applied (there was no available data to derive set of characterization factors that would be consistent with existing impact categories, such as ecotoxicity) (Publication II).

4.2. Characterization of BR valorization streams from a radiological perspective

4.2.1. Radionuclide mass flow within the Bayer process

Prior to analysis of the BR valorization processes, a specific study has been conducted to characterize radionuclide mass flow within the Bayer process using Mytilineos S.A. aluminum plant as a reference and a source of sample materials (Publication IV). Measurements have considered inventory materials (different bauxites and lime) as well as midpoint materials and output products and residues. ^{40}K, two long lived radionuclides from thorium decay chain (^{228}Ra and ^{228}Th) and two from uranium chain (^{238}U and ^{226}Ra) were measured. Various long-lived nuclides from thorium and uranium decay chains were selected as their chemical properties and behavior during processing might differ.

It was demonstrated that karst bauxites (from Greece and Turkey, roughly 80% of the feed material) have considerably higher content of natural radionuclides compared to lateritic bauxites (from Ghana and Brazil): 1.7–2.4 times higher for ^{238}U series nuclides and 1.4–2.0 times higher for ^{232}Th series nuclides. ^{40}K remained below minimum detectable amount for lateritic bauxites, while for karst bauxite coming from Turkey it was 10–20 times higher than for different karst bauxites from Greece, see **Table 5**. Bauxites coming from Greece were mined from different locations at the Parnassos-Ghiona area by different suppliers and thus are represented by different entries.

Table 5: Activity concentration of different bauxites used by Mytilineos S.A. Measurement uncertainties are reported at the confidence level of 2σ.

Material and description	Activity concentration [Bq/kg d.w.[2]]				
	^{228}Ra	^{228}Th	^{238}U	^{226}Ra	^{40}K
Trombetas bauxite (lateritic bauxite, Porto Trombetas, Brazil)	129 ± 4	129 ± 6	36 ± 3	37 ± 1	<9
Ghana bauxite (lateritic bauxite, Awaso, Ghana)	112 ± 3	112 ± 5	34 ± 3	36 ± 1	<9
Turkish bauxite (karst bauxite, Taurides range an Milas area, Turkey)	181 ± 5	181 ± 9	99 ± 7	108 ± 2	103 ± 6
High silica bauxite (karst bauxite, Parnassos-Ghiona area, Greece)	189 ± 5	182 ± 9	97 ± 6	95 ± 2	5 ± 4
S&B bauxite (karst bauxite, Parnassos-Ghiona area, Greece)	188 ± 5	184 ± 9	85 ± 6	87 ± 2	8 ± 4
Delphi Distomo bauxite (karst bauxite, Parnassos-Ghiona area, Greece)	228 ± 6	223 ± 11	60 ± 4	70 ± 1	10 ± 4

[2] d.w. – dry weight

The radionuclide flow for every specific isotope is presented in Figures 9–13, where the results are presented in the form of normalized activity [Bq/kg] over a mass of aluminum hydroxide flow on a daily basis as in the equation 16. *n/a* notion is used whereas the samples were not available. This is specific to the slurry which is a mixture of solid and liquid phases. During sampling only solid fraction was extracted and then measured. In case isotope concentration was below Minimal Detectable Amount (MDA), the measured MDA value was substituted into the equation 16 instead, and values below MDA were provided

$$Normalized\ Activity = \frac{Sample\ activity \times Daily\ mass\ flow}{Aluminium\ hydroxide\ mass\ flow} \tag{16}$$

$$I.E. = \frac{C_{BR}}{\sum C_{bauxite} \cdot bauxite\ mass\ fraction} \tag{17}$$

The black lines stand for solid material mass-flow, orange for liquid and dashed lines for mixtures (referred to as slurry). Karst bauxite comprises of the mixture of all the karst bauxites from Table 5 with radionuclide concentration measured and reported in the top right corner of Figures 9–13. Only one lateritic bauxite is usually used at a time (either From Ghana or Brazil) and during sampling period bauxite from Trombetas in Brazil was used. Isotope enrichment ratio to BR corresponds to the concentration increase of a specific radionuclide (C_{BR}) within BR over mass-normalized concentration of this radionuclide in the initial bauxites as described in equation 17.

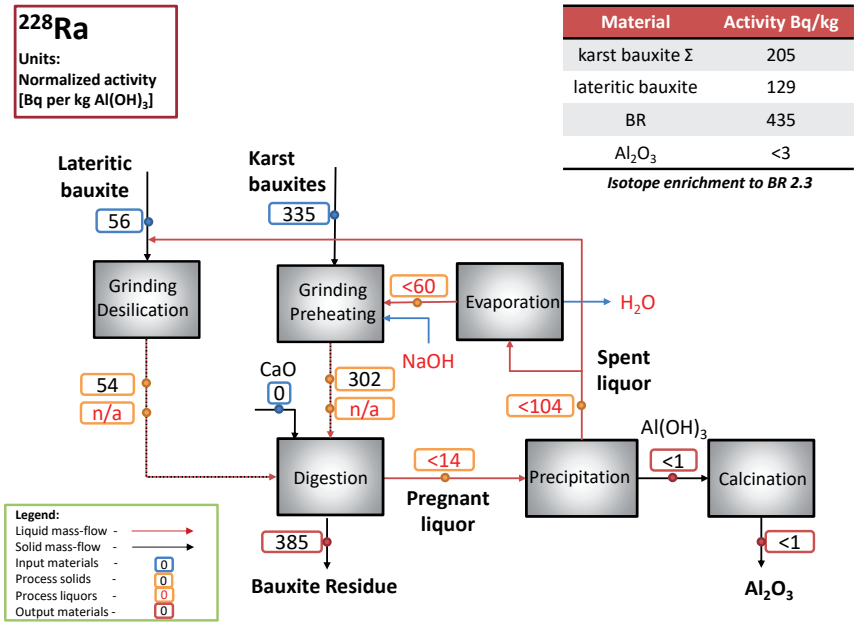

Figure 9: ^{228}Ra (product from thorium decay series) mass-flow through Bayer process.

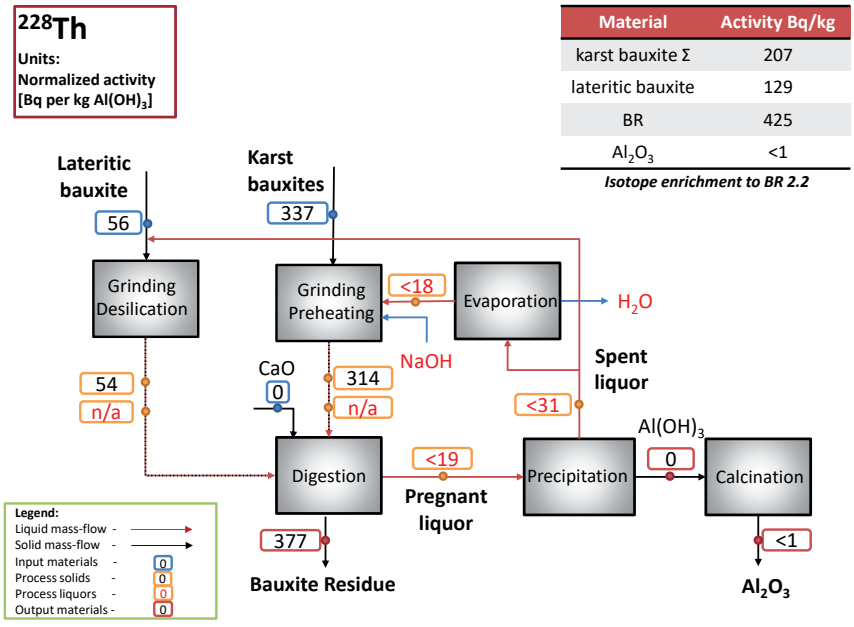

Figure 10: ^{228}Th (product from thorium decay series) mass-flow through Bayer process.

For thorium decay chain, daughter nuclides ^{228}Ra (**Figure 9**) and ^{228}Th (**Figure 10**) behaved in the same way. Initially karst and lateritic bauxites were dissolved in the process liquors and measured isotope flows were slightly diluted. Then, all these radionuclides ended up in the BR and no evidence of the dissolution of these two nuclides in the process liquors or entering alumina were observed.

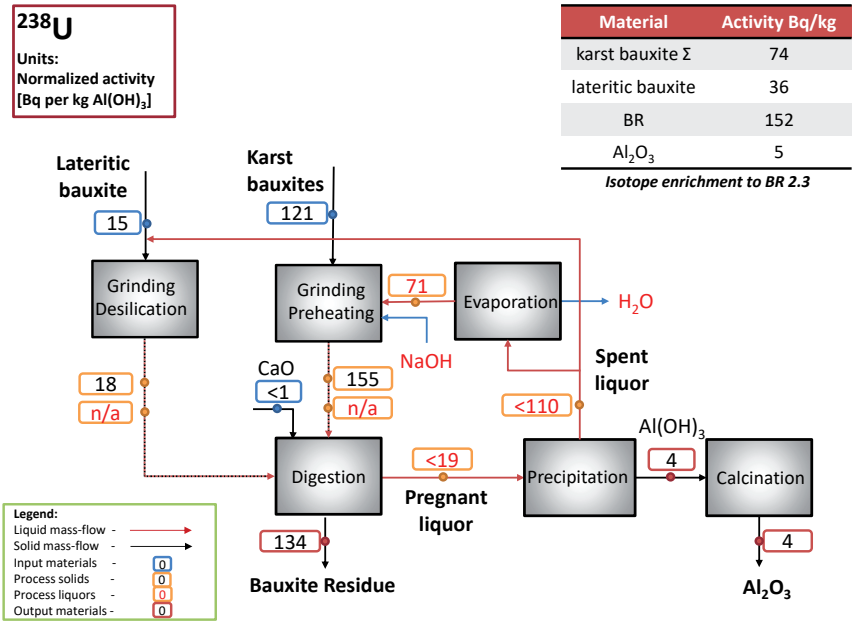

Figure 11: ^{238}U mass-flow through Bayer process.

Dissolution of ^{238}U (**Figure 11**) in the process liquor took place, as well as minor portion of this isotope was detected in the alumina. Measured activity concentration of 4 Bq/kg in the $Al(OH)_3$ and 5 Bq/kg in the Al_2O_3 are in agreement with the results found in the literature [69], [70]. High MDA values in pregnant and spent liquors are attributed to the 63.3 keV gamma line of ^{234}Th. Low energy of this gamma photon makes self-absorption effect in the measurement sample too prominent, thus reducing number of photons reaching the detector. Combined with low quantities of measured isotope, this gives larger measurement uncertainty.

These results are presented to enhance scientific understanding; the detected values in the alumina are below natural background and are too low to have radiological implications for processing.

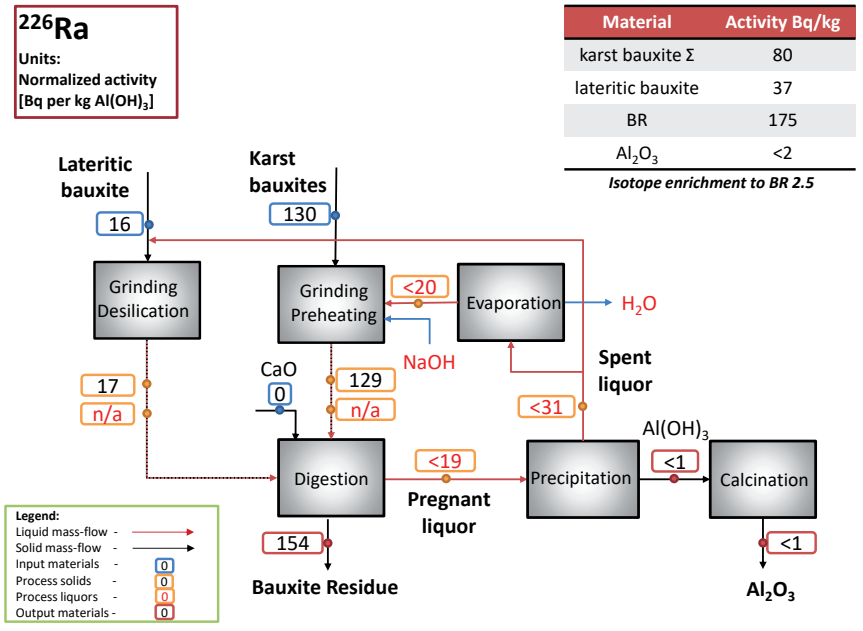

Figure 12: ^{226}Ra (product from uranium decay series) mass-flow through Bayer process.

^{226}Ra (decay product of ^{238}U, **Figure 12**) behaved in a similar way to ^{228}Ra and ^{228}Th: it did not dissolve in the process liquors and all the activity concentration ended up in the bauxite residue. The fact that ^{238}U and ^{226}Ra behave differently is an example of a broken equilibrium chain.

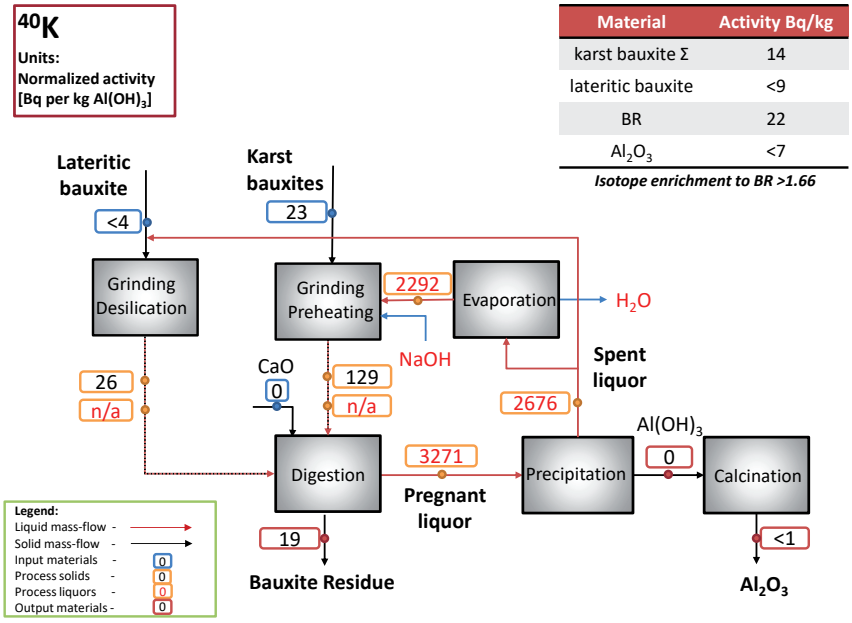

Figure 13: ^{40}K mass-flow through Bayer process.

A considerable accumulation of ^{40}K (see **Figure 13**) was observed in the process liquors, however this isotope was not detected in the alumina. Presented high ^{40}K values in the process liquors are attributed to the fact, that figures demonstrate mass normalized activity as described in equatioin16 and high volume of liquor material passing through the process. The real measured ^{40}K concentrations in the process liquors were as follows: (290 ± 20 Bq/kg in pregnant liquor, 260 ± 30 Bq/kg in spent liquor, 310 ± 30 Bq/kg in concentrated (after evaporation stage) liquor). Activity concentration remained below EU BSS screening limit set to 10 000 Bq/kg for this isotope [14].

It was observed that ^{40}K isotope is dissolved in the Bayer process, however there is no evidence that it precipitates into alumina. The ^{40}K content in BR showed a slight decrease compared to initial quantities entering with bauxites (isotopic enrichment in the BR was found to be >1.66, whereas for other measured isotopes it remined in the range of 2.2–2.5). Tests have been performed to check whether this element might settle in the form of scales in the evaporation, digestion or preheating tanks, however scale analysis did not confirm this hypothesis (Publication IV). Further studies would be needed to better understand the fate of this radionuclide.

Overall, the mass balance closed for 4 (^{228}Ra, ^{228}Th, ^{238}U, ^{226}Ra) out of 5 studied radionuclides. The discrepancies between outputs and inputs for ^{40}K cannot be explained purely by measurement uncertainties or data quality and therefore further research is needed to explain observed phenomena.

Bauxite residue was confirmed to be accumulation point for most radionuclides entering the Bayer process, even though dissolution of ^{238}U and ^{40}K was

observed in the process liquors. It was concluded that at any given processing stage of the process at the specific plant, materials that could be potentially hazardous for people from the radiological perspective are not formed. The exact measured activities and further description of the findings are provided elsewhere (Publication IV). However, the results and conclusions are valid for specific bauxite types processed at a single alumina plant and these results should not be extrapolated to other facilities, as conditions and radionuclide concentrations there might differ significantly.

4.3. Construction materials produced with bauxite residue

4.3.1. Inorganic polymers and infrastructural exposure

To prepare inorganic polymers, initial BR (88.56% d.w.) was mixed with carbon (1.44% d.w.) and silica (10% d.w.) sources and fired at temperature 1200 °C. Resulting precursor material was then mixed with different activating solutions: potassium (solution to precursor ratio: 0.25) and sodium (solution to precursor ratio: 0.15) silicate (Publication III). The mixture was then molded into pavement blocks. The activity concentration was then measured for two resulting materials and activity concentration index was calculated as reported in **Table 6**. Potassium silicate activated mixture (K-silicate) had lower content of ^{226}Ra and ^{232}Th due to higher dilution ratio of BR compared to the sodium silicate activated solution (Na-silicate), while had considerably higher content of ^{40}K isotope coming from the natural potassium. The resulting ACI is 2.5 for K-silicate and 2.3 for Na-silicate were above the limit for the dwelling usage (ACI < 1), while well below limit for infrastructural applications (ACI < 6).

Table 6: Activity concentration measured in different pavement blocks. Measurement uncertainties are reported at the confidence level of 2σ.

Activating solution	Activity concentration [Bq/kg d.w.]			Activity concentration index (ACI)
	^{226}Ra	^{232}Th	^{40}K	
K-silicate	139 ± 2	341 ± 4	889 ± 20	**2.5**
Na-silicate	147 ± 3	366 ± 7	48 ± 19	**2.3**

The impacts on the different LCA categories are discussed elsewhere (Publication III), while this study focuses only on the NORM an artificial radionuclides impact categories. These results are summarized in the **Table 7** for the NORM impact category and in the **Table 8** for artificial radiation. The overall comparison shows that 98.9% of the human exposure takes place during the use phase, which is logical as then the radionuclides are in the vicinity of humans and exposing them. Slightly higher total exposure from the potassium silicate pavement blocks is

explained by the rather high content of potassium, which contains natural radioactive isotope ^{40}K. The raw material, processing and end of life stages here do not consider occupational exposure as this can be deemed as negligible but instead focus on the release of natural radionuclides into the environment (mining activities, energy production from fossils).

It should be noted that the levels of the exposure remain well below radiological limits and that any conventional pavement blocks produced without BR would also incorporate some quantities of naturally occurring radionuclides as these are abundant in the raw materials.

Table 7: Impact from natural radionuclides from the 1 m^2 (5 cm thick) paving blocks per life cycle stage

Material	**Dose [man.Sv/m^2 paving]**				
	Raw materials	Processing	Use phase	End of life	**Total**
K-silicate	1.10×10^{-8}	4.72×10^{-8}	5.35×10^{-6}	9.33×10^{-11}	5.41×10^{-6}
Na-silicate	5.17×10^{-9}	5.24×10^{-8}	5.12×10^{-6}	9.51×10^{-11}	5.18×10^{-6}
	Percentage contribution				
K-silicate	0.2%	0.9%	98.9%	0.0%	**100%**
Na-silicate	0.1%	1.0%	98.9%	0.0%	**100%**

Table 8: Impact from artificial radiation from the 1 m^2 (5 cm thick) paving blocks per life cycle stage

Material	**Dose [man.Sv/m^2 paving]**				
	Raw materials	Processing	Use phase	End of life	**Total**
K-silicate	9.68×10^{-9}	3.77×10^{-8}	–	1.24×10^{-10}	$\mathbf{4.75 \times 10^{-8}}$
Na-silicate	4.24×10^{-9}	4.20×10^{-8}	–	1.26×10^{-10}	$\mathbf{4.64 \times 10^{-8}}$
	Percentage contribution				
K-silicate	20.4%	79.4%	–	0.3%	**100%**
Na-silicate	9.1%	90.5%	–	0.3%	**100%**

When NORM exposure is compared to the impact of the artificial radionuclides (presented in Table 8), it can be concluded that the impacts are highly similar in most of the lifecycle stages, with the exception of the use phase – artificial radionuclides come from the nuclear fuel cycle and their exposure is a part of energy mix. These nuclides do not end up in the final products, contrary to the natural nuclides, but are mainly associated with the energy consumed during different life-cycle stages.

4.3.2. Bauxite Residue added to cement

In the current study, the ACI (see section 3.2.2) is used to compare different types of cements, thus assumption would be made that for the concrete preparation the same ratios of components would be used. This is not always the case; however, it would allow us for qualitative comparison of different materials. The simplified flowchart for cement production is presented in **Figure 14**. Typical pozzolans used in the cement industry are: metakaolin, silica fume, fly ash or metal slags. The latter two come as byproducts from other industrial processes and often have elevated natural radionuclide content.

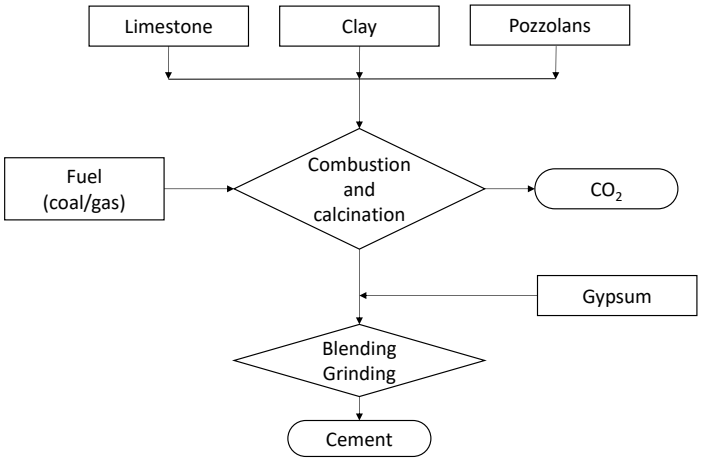

Figure 14: Portland cement general production inventory flow.

Four types of industrially produced cements are presented in the **Table 9** (samples were provided by TITAN Cement Company S.A., Greece) as well as corresponding activity concentration indexes (ACI) are calculated. Mean radionuclide content in average Greece and EU cements is provided for comparison. The ACI of the cement samples coming from TITAN cement plant remain slightly below the average EU and Greek cement samples. Among the four samples from TITAN plant, CEM II/B-M (W-P-LL) 32,5N has the highest concentration of every analyzed radionuclide. This is explained by the addition of the fly ash, which is a product of coal burning and accumulates iron and alumina desirable for the construction industry, while also unwanted radionuclides. The activity concentration of fly ash used in this cement plant has previously been characterized to be 800 Bq/kg ^{226}Ra (^{238}U decay chain), 53 Bq/kg ^{228}Th (^{232}Th decay chain) and 800 Bq/kg 40K [71]. Yet, fly ash is widely and safely utilized in cement production.

Table 9: Radionuclide concentrations and ACI in different cement types. Measurement uncertainties are reported at the confidence level of 2σ.

Cement	Activity concentration [Bq/kg d.w.]			Activity concentration index (ACI)
	^{226}Ra	^{232}Th	^{40}K	
CEM I 42.5R[3]	22 ± 1	17 ± 1	140 ± 10	**0.2**
CEM I 52,5N	22 ± 1	17 ± 1	139 ± 10	**0.2**
CEM II/A-M (P-LL) 42,5N	35 ± 1	16 ± 2	166 ± 10	**0.3**
CEM II/B-M (W-P-LL) 32,5N	85 ± 2	25 ± 2	252 ± 14	**0.4**
Greece average (based on 183 samples) *[63]*	85	19	257	**0.5**
EU average (based on 2013 samples) *[63]*	45	31	216	**0.4**

Next, multiple BR containing cements have been prepared and their activity concentration was compared to the standard OPC (CEM I 42.5R) as in **Table 10**. Please note that OPC standard (CEM I 42.5R) samples are reported both in **Table 9** and **Table 10** with different radionuclide concentrations. These are different samples of the same cement time, which demonstrate fluctuation of the radionuclides coming from the feed materials. However, this remains insignificant and the ACI remains the same – 0.2.

Table 10: Cements produced with the addition of BR. Measurement uncertainties are reported at the confidence level of 2σ.

Cement	Activity concentration [Bq/kg d.w.]			Activity concentration index (ACI)
	^{226}Ra	^{232}Th	^{40}K	
OPC standard (CEM I 42.5R)	20 ± 1	21 ± 1	94 ± 9	**0.2**
S1 OPC standard (with 2.3% BR)	24 ± 1	35 ± 2	94 ± 8	**0.3**
S2 OPC extreme (with 8.1% BR)	33 ± 1	58 ± 2	29 ± 5	**0.4**
S3 BR rich cement (55% BR)	114 ± 2	252 ± 8	28 ± 6	**1.6**
S4 BR rich cement (65% BR)	129 ± 2	292 ± 10	3 ± 6	**1.9**

[3] CEM I is 100% Ordinary Portland Cement (OPC). CEM II is OPC mixed with additives. Number stands for compressive strength [MPa], R = early strength gain, N = normal strength gain. A = additive content < 20%. B = additive content > 20%. M = multiple additives are used. P = pozzolan. LL= limestone < 0.2%. W = fly ash.

Samples S1 and S2 were prepared with low BR content replacing portion of pozzolana materials with BR. Increase in the measured radionuclide content and ACI does not have any implication on the radiological hazardousness as the materials remain safe and the ACI stays below average ACI in Greek cement samples presented in the **Table 9**. Previous studies have confirmed that utilizing up to 5% BR in the raw material feed does not have impact on the thermal behavior of the materials and gives compressive strength above 53 MPa after 28 days, which classifies them as CEM I 52,5N category [62].

Samples S3 (BR: 55%, limestone 20%, gypsum 25%) and S4 (BR: 65%, limestone 15%, gypsum 20%) have demonstrated considerable radionuclide increase and the ACI has exceeded screening value of 1, making them potentially unsuitable for mass use in the construction of living premises. However, if used for infrastructure or in limited amounts for dwellings these BR rich cements would pose no radiological hazard and would help solving problem of mass utilization of the BR. It should be noted that the radionuclide concentration could be diluted in the preparation of concrete (where cement is only one of the constituents). Mechanical tests for samples S3 and S4 have demonstrated 28-day compressive strength of 29.1 MPa and 26.3 MPa respectively, which makes them inferior to OPC. Such materials can still have different commercial applications which are discussed elsewhere [72].

4.4. Bauxite residue valorization: residue stream characterization.

BR valorization is currently considered economically unfeasible, when compared to conventional metal recovery methods. However, development of a multistage process might serve as a potential alternative, considering recovery of multiple valuable metals. Additionally, assigning the cost to recovery of residues or increasing economic burden on landfilling can serve as an extra measure to motivate valorization.

Sections 4.4.1 and 4.4.2 provide a summary of the valorization byproducts obtained by various BR processing techniques based on the number of processing steps. Results presented in the **Table 11** and **Table 12** were directly produced from the BR, while **Table 13** presents results of a two stage valorization process: first, iron was recovered with reduction smelting and then other metals were extracted. More detailed measurement results are provided elsewhere (Publications V–VI), while here only accumulation ratio is presented.

4.4.1. Single stage valorization

Reduction smelting is an efficient way to recover iron (~46% of Greek BR comprises of Fe_2O_3) from BR, which can potentially lead to high radionuclide accumulation. This can be compensated for by the amounts of fluxing materials (feed materials that are added to facilitate the removal of impurities from raw materials). In the current experiments flux to BR ratio varied from zero (i.e., no flux was used resulting in the highest radionuclide accumulation in the slag) to 1:10, which explains high variability in the radionuclide accumulation ratios. A single sample exceeded EU BSS [14] screening value of 1000 $Bq \cdot kg^{-1}$ for ^{228}Th (1013 ± 32 $Bq \cdot kg^{-1}$ for the sample with no fluxes added (Publication V)), while the rest remained below screening boundaries. Overall, radionuclide concentration in the slag residue was inversely proportional to the amounts of flux materials added and most of the radionuclides are expected to end up in the slag residue, however, no experiments with the recovered pig iron have been performed.

Table 11: Radionuclide accumulation in the secondary residues produced after single-stage valorization process.

Process	Number of experiments	Nuclide	AR range	Mean AR
Reduction smelting of iron	10	^{226}Ra	1.4–2.3	1.8
		^{228}Ra	1.2–2.1	1.6
		^{228}Th	1.3–2.5	1.7
Reduction roasting of iron	1	^{226}Ra	1.1	–
		^{228}Ra	1.1	–
		^{228}Th	1.0	–
Alkali leaching of alumina	9[4]	^{226}Ra	1.1–1.3	1.2
		^{228}Ra	1.1–1.2	1.2
		^{228}Th	1.2–1.4	1.3
Acidic metal recovery	3	^{226}Ra	1.2	1.2
		^{228}Ra	1.1–1.2	1.2
		^{228}Th	1.1–1.3	1.2
Ionic liquid leaching	9	^{226}Ra	1.1–1.9	1.4
		^{228}Ra	1.0–1.5	1.2
		^{228}Th	0.8–1.3	1.1

[4] 9 Samples from different experiments were mixed and measured in 2 batches due to low sample mass (0.1–1 g)

Reduction roasting is an alternative method for iron separation. With this method only a single experiment was analyzed, and results separately summarized in the **Table 12**. Samples Magnetic I and II correspond to recovered magnetic iron that has previously been converted to the magnetic form using roasting process and remaining materials are left as residue.

The residue itself does not pose any significant radionuclide accumulation (maximum AR 1.1), while considerable radionuclide accumulation is observed in the recovered magnetic iron (both samples). The word 'accumulation' might not be the proper one for the recovered magnetic iron, as this is valorized material fraction, however, it provides understanding of the radionuclide content change compared to the initial BR. This leads to an observation that a significant portion of radionuclides in the currently studied BR might be associated with iron. As a result, upscaling of such a process would require further investigation of the radionuclide behavior and associated radiological hazards.

Table 12: Radionuclide accumulation ratio in different process stages of the reduction roasting process.

Process	Nuclide	Magnetic I	Magnetic II	Residue
Reduction roasting	^{226}Ra	1.5	1.5	1.1
	^{228}Ra	1.5	1.4	1.1
	^{228}Th	1.6	1.4	1.0

Residues coming from the alkali leaching process were too small (0.1–1 gram) and therefore had to be mixed together to give a larger sample mass. As a result, samples from 9 leaching experiments were mixed into 2 measurement batches to be used in gamma-ray measurements. Resulting radionuclide accumulation ranged between 1.1–1.4, with mean radionuclide content increase by a factor of 1.2–1.3.

During acidic metal recovery, iron, alumina, titanium and REE were dissolved in acids. Valuable metals recovery usually stayed within 20–60% range from the initial content of these metals in the BR [21]. However, the mean radionuclide accumulation ratio was observed to be 1.2, meaning that potentially, a considerable quantity of radionuclides was also dissolved by acids. This should be confirmed by future studies.

Ionic liquid residues were obtained after dissolving and recovering primary metals and REE with [Emim][HSO_4]. Overall, this ionic liquid has a potential for 100% recovery of iron, >90% recovery of titanium and ~80% of scandium [27]. Residues from 9 experiments were analyzed, experimental conditions varied (solid to liquid ratio, settling time, stirring rate and heating temperature). This had a significant effect on the radionuclide content in the solid residues: accumulation rate varied in the range of 1.1–1.9 for ^{226}Ra, 1.0–1.5 for ^{228}Ra and 0.8–1.3 for ^{228}Th. Residues show distinct difference between accumulation rate of radium isotopes (^{226}Ra, ^{228}Ra) and ^{228}Th, where the latter shows considerably lower accumulation rate and in some cases the thorium content in the newly produced

residue samples was lower than in the initial BR. It is evident that a significant portion of thorium was dissolved and is recovered altogether with valuable metals.

4.4.2. Two-stage valorization

A set of experiments were conducted with the reduction smelting slag (BR, after recovery of iron using limestone as a flax material), see **Table 13**. In this case experiments were conducted with larger material masses and residue masses were 1–3 grams, thus every sample was measured separately without mixing. New samples obtained after recovery of alumina with alkali leaching show mean accumulation ratio 1.2–1.3, similar to the alumina recovery from BR itself (see **Table 11**). This is an interesting observation, as there is no significant radionuclide buildup in the residue obtained after 2 stages of valorization.

Table 13: Radionuclide accumulation in the secondary residues produced after single-stage valorization process (pre-treated BR is an input material).

Process	Number of experiments	Nuclide	Mean accumulation in slag[5]	AR range	Mean AR[6]
Alkali leaching of alumina	6	^{226}Ra	1.4	1.2–1.4	1.3
		^{228}Ra	1.2	1.1–1.2	1.2
		^{228}Th	1.3	1.3	1.3
Acidic metal recovery	6 (HCl)	^{226}Ra	1.7	0.4–0.9	0.7
		^{228}Ra	1.5	0.2–0.8	0.6
		^{228}Th	1.6	0.8–3.1	1.6
Acidic metal recovery	5 (H_2SO_4)	^{226}Ra	1.7	0.8–1.4	1.2
		^{228}Ra	1.5	0.6–1.3	1.0
		^{228}Th	1.6	0.7–1.2	0.9

Residue samples produced after acidic metal recovery were divided into two groups based on the acid used, as different accumulation behavior was observed for HCl and H_2SO_4. The HCl leaching process has resulted in a rather efficient recovery of radium radionuclides and therefore enrichment ratios <1 in all of the experiments. It was also confirmed by studying liquid leach liquor samples (Publication VI), which contained significant amounts of ^{226}Ra and ^{228}Ra isotopes. This raises a radiological concern, for the chemical industry, on how to ensure worker safety and how to separate hazardous radionuclides, however, this topic is to be covered in future studies. ^{228}Th demonstrated lower solubility with

[5] Iron was recovered from BR with the reduction roasting process and slag was resulting residue, which then was used at the next stage of valorization process.

[6] Accumulation rate is relative to the initial BR.

the HCl acid and its concentration in the residue samples always remained higher than for radium isotopes, reaching 1645 ± 36 and 1250 ± 26 Bq/kg. Conservative radiological modeling has demonstrated that even though EU BSS screening limit is exceeded, there would be no risk of elevated radiological exposure to workers once the production is upscaled (Publication IV).

Leaching with H_2SO_4 acid resulted in a more varying radionuclide behavior: in some of the experiments radionuclide concentration in the residue decreased to the levels of initial BR, in some it increased. This was also confirmed by the measurements of the liquid leachate liquor samples, which had significant concentrations of all three radionuclides. All three isotopes have demonstrated high variability in the activity concentration, thus strongly depending on the experimental conditions. It is not common to include consideration of the radionuclide concentrations into the design of the chemical processes; however current results indicate that such considerations might be needed due to high rate of radionuclide co-recovery. This remains a topic for future studies.

5. SUMMARY AND CONCLUSIONS

This thesis focuses on two main aspects of natural radioactivity in industrial residues: (1) development of NORM impact categories for the LCA methodology, (2) analysis from the radiological perspective of different BR valorization chains that include production of construction materials and development of new metal recovery techniques.

First, it is important to note that the activity concentrations observed in the current study are too low to be classified as measurably hazardous to humans. The possible doses coming from these materials would be comparable to or below background levels of radiation, and there is insufficient evidence to associate these potential doses with elevated health risks. However, it should be kept in mind that some NORM radionuclides are chemically toxic, and it might be worthwhile to assess their potential toxicological impact in addition to the radiological impacts considered in this thesis.

Secondly, author would like to remind that the measurement results are specific to the sites that provided samples for measurement (Mytilineos S.A. aluminum plant and TITAN Cement Company S.A. from Greece). Conclusions might be different for other facilities, as the processes or inventory materials might differ significantly.

5.1. NORM-LCA methodology development

In general, it is believed that waste management and recycling is beneficial to society. However, there is the potential of burden shifting from one impact category to another or overlooking certain important impacts when developing novel industrial processes. To get a clear picture, LCA methodology is often used to assess impacts from a product or a process from the cradle to the grave in a set of different environmental and human related categories. When valorizing BR, such assessments are also needed. However, this material may contain natural radionuclides which have not been covered so far by LCA methodologies. To fix this shortcoming, NORM-LCA impact category has been developed during current study.

Newly developed NORM-LCA impact categories have been used to assess impacts of natural radionuclides coming from the decay chains of ^{238}U and ^{234}Th, and from ^{40}K to human and biota species.

The overall damage to humans in the NORM-LCA impact category was rather similar for the different scenarios studied. The introduction of BR into cement and fired bricks was found to exhibit for human exposure an acceptable increase, which is a minor effect and well-correlated with the condition that conventional construction materials can already contain certain amounts of natural radionuclides.

An indirect benefit from the developed NORM-LCA impact category was the characterization of impacts coming from isotopes that were already included in existing LCA databases (for instance ^{210}Pb coming from cement industry or ^{210}Pb and ^{210}Po coming from coal fired power plants). A notable observation is that potential health effects linked to natural radionuclides occasionally present in some conventional building materials accounted for the largest share of overall impacts measured in the study. This finding underlines the importance of looking at environmental problems as a whole to get a clear picture of certain activities and to avoid overlooking risks and damage coming from activities that are generally regarded as benevolent (like waste recycling).

Analysis of NORM impact on the environment has demonstrated that the largest impact is associated with BR landfilling, which is expected, as this action may readily transfer radionuclides to the recipients. However, derived impact factors have limited applicability. Firstly, derived damage units of PDF·m^3·day do not show direct damage to biota species (unlike DALY in human impact category) but provide a surrogate tool for qualitative comparison. Secondly, cross-comparisons with other impact categories were not performed, as a different method of deriving impact factors was used due to limited data available.

5.2. Construction materials

The utilization of BR in the construction sector can potentially lead to reductions in waste volumes and fewer landfill sites. At the same time, the consideration of radiological safety of construction materials incorporating BR is recommended due to the natural radionuclides present in some BR samples. Radiological exposure is a consideration for both conventional and novel construction materials, as some existing construction materials already may contain some quantity of natural radionuclides. The BR materials considered in this study for construction applications were found to exhibit only minor radiological characteristics; the activity concentrations observed were too low to be classified as measurably hazardous to humans, with insignificant effects compared to existing construction materials.

It has been demonstrated that utilizing low BR quantities in OPC can be achieved without altering materials mechanical or radiological properties. However, this does not help solve the problem of vast streams of BR production. Increasing fraction of BR can potentially help reduce volumes of landfills, however, this could lead to reduction of compressive strength compared to conventional cement types.

Inorganic polymer materials can potentially solve this issue. These materials can be prepared with BR content above 50% while still having desired mechanical properties. However, radionuclide content in such materials leads to the ACI above 1 and therefore such materials can have limited application in the construction of dwellings or use in infrastructural applications. It should also be mentioned that the focus of the current study was mainly on the impacts of

ionizing radiation; therefore, this work has not included a chemical toxicity assessment for any potentially hazardous elements which may theoretically be present in BR. In summary, there is a balance to be achieved in selecting the optimal BR content in construction materials incorporating BR; it is important to find a BR concentration that guarantees desirable mechanical and radiological properties, while simultaneously meeting requirements for potential reductions in BR storage sites.

5.3. BR valorization

From a process engineering standpoint, the detected radiological values associated with BR valorization for the studied samples have been demonstrated to be below natural background and are accordingly too low to have radiological implications for processing. Potential reasons for these findings are: (1) addition of diluting materials like lime in the reduction smelting process; (2) extraction of radionuclides with the valuable metals recovered (reduction roasting, acidic leaching, and ionic liquid leaching). This has been confirmed also for multi-stage valorization chains.

It was confirmed that the equilibrium decay chains of natural uranium and thorium can be broken and isotopes from a single chain would end up in different products: (1) during Bayer process ^{238}U is dissolved and minor portion of this isotope reaches aluminum, while ^{226}Ra remains in solid form and its quantity ends up in BR, (2) dissolution of BR in HCl acid after iron recovery has shown strong recovery of radium isotopes (^{226}Ra and ^{228}Ra) with valuable metals, while ^{228}Th mostly ended up in the final residue.

6. OUTLOOK

In this work, the environmental impact category for the NORM-LCA methodology has been developed based on the considered NORM materials and the current state-of-the-art knowledge of the ionizing radiation impact on biota species. However, this knowledge is limited and thus resulted in model limitations. A further model update would be needed once more data and knowledge are gathered on this topic.

This thesis has examined the introduction of BR into construction materials from a radiological exposure perspective. Future studies would be recommended to assess the impacts of potential chemically hazardous elements which may have been introduced into the novel materials. This could be achieved by leaching tests to measure the releases to the environment from these materials.

Multiple BR valorization techniques have been associated with the co-recovery of radionuclides (reduction roasting, acidic leaching, and ionic liquid leaching). Further studies are needed to further analyze radionuclides recovered with valuable metals and to confirm that these processes can be safely upscaled to pilot plant or industrial levels without any harm posed by ionizing radiation. It is suggested that further studies are carried out in connection with mineral analysis, to connect solubility and co-recovery of the radionuclides with the mineral phases, where these radionuclides occur.

A minor discrepancy in the quantities of ^{40}K in the Bayer process was observed: the feed flow of this nuclide was bigger than the sum of outflows. It was evident that ^{40}K is accumulated within process liquors, however, final fate of this nuclide remained unexplained. Further research activities are needed to confirm whether this behavior can be attributed to measurement or other uncertainties, the formation of ^{40}K rich scales, or any other phenomena.

REFERENCES

[1] International Aluminium Institute (IAI), "Bauxite Residue Management: Best Practice," Sep. 2014. Accessed: May 20, 2025. [Online]. Available: https://aluminium.org.au/wp-content/uploads/2017/10/Bauxite_Residue_Management_-_Best_Practice_(IAI).pdf

[2] K. Evans, "The History, Challenges, and New Developments in the Management and Use of Bauxite Residue," *Journal of Sustainable Metallurgy*, vol. 2, no. 4, pp. 316–331, 2016, https://doi.org/10.1007/s40831-016-0060-x.

[3] K. Evans, "Successes and Challenges in the Management and Use of Bauxite Residue," in *BR2015Proceedings_for_Print*, Leuven, Oct. 2015, pp. 1–16. Accessed: Mar. 28, 2025. [Online]. Available: https://conference2015.redmud.org/wp-content/uploads/2015/10/Ken-EVANS-secure.pdf

[4] "Statiscal data published at the World Aluminium webpage." Accessed: Nov. 21, 2018. [Online]. Available: http://www.world-aluminium.org/statistics/#data

[5] G. Bardossy, *Karst Bauxites-Bauxite Deposits on Carbonate Rocks*, vol. 14. Developments in Economic Geology, Elsevier, 1982. *https://doi.org/*10.1016/c2009-0-14505-1.

[6] G. Bardossy and G. J. J. Aleva, *Lateritic Bauxites*. Development in Economic Geology, Elsevier, 1990.

[7] G. Mucsi, B. Csoke, and K. Solymár, "Grindability characteristics of lateritic and karst bauxites," *Int J Miner Process*, vol. 100, no. 3–4, pp. 96–103, 2011, https://doi.org/10.1016/j.minpro.2011.05.006.

[8] A. R. Hind, S. K. Bhargava, and S. C. Grocott, "The surface chemistry of Bayer process solids: A review," *Colloids Surf A Physicochem Eng Asp*, vol. 146, no. 1–3, pp. 359–374, 1999, https://doi.org/10.1016/S0927-7757(98)00798-5.

[9] I. Paspaliaris, D. Panias, and C. Skoufadis, "Precipitation and Calcination of Monohydrate Alumina From the Bayer Process Liquors," in *Third annual workshop Eurothen 2000*, Jan. 2000, pp. 539–556.

[10] G. Power, M. Gräfe, and C. Klauber, "Bauxite residue issues: I. Current management, disposal and storage practices," *Hydrometallurgy*, vol. 108, no. 1–2, pp. 33–45, 2011, http://dx.doi.org/10.1016/j.hydromet.2011.02.006.

[11] S. Ruyters, J. Mertens, E. Vassilieva, B. Dehandschutter, A. Poffijn, and E. Smolders, "The red mud accident in Ajka (Hungary): Plant toxicity and trace metal bioavailability in red mud contaminated soil," *Environ Sci Technol*, vol. 45, no. 4, pp. 1616–1622, 2011, https://doi.org/10.1021/es104000m.

[12] R. L. Burritt and K. L. Christ, "Water risk in mining: Analysis of the Samarco dam failure," *J Clean Prod*, vol. 178, pp. 196–205, 2018, https://doi.org/10.1016/j.jclepro.2018.01.042.

[13] Frik Els, "Major tailings dam burst reported in China," Mining.com. Accessed: Mar. 28, 2025. [Online]. Available: https://www.mining.com/major-tailings-burst-reported-in-china/#:~:text=China%20has%20nearly%208%2C000%20tailings,partially%20destroyed%20a%20nearby%20town.

[14] European Parliament, "Council Directive 2013/59/Euratom of 5 December 2013 laying down basic safety standards for protection against the dangers arising from exposure to ionising radiation, and repealing Directives 89/618/Euratom, 90/641/Euratom, 96/29/Euratom, 97/43/Euratom a," *Off J Eur Commun L13*, no. December 2003, pp. 1–73, 2014.

[15] UNSCEAR, “Sources and Effects of Ionizing Radiation,” New York, 2000. Accessed: Mar. 28, 2025. [Online]. Available: https://www.unscear.org/docs/publications/2000/UNSCEAR_2000_Report_Vol.I.pdf
[16] ICRP, “The 2007 Recommendations of the International Commission on Radiological Protection. ICRP Publication 103.,” *Ann ICRP*, vol. 37, no. 2–4, pp. 1–332, 2007, Accessed: Mar. 28, 2025. [Online]. Available: https://journals.sagepub.com/doi/pdf/10.1177/ANIB_37_2-4
[17] IAEA, “Extent of Environmental Contamination by Naturally Occurring Radioactive Material (NORM) and Technological Options for Mitigation,” Vienna, 2003. Accessed: Mar. 28, 2025. [Online]. Available: https://www.iaea.org/publications/6789/extent-of-environmental-contamination-by-naturally-occurring-radioactive-material-norm-and-technological-options-for-mitigation
[18] R. M. Rivera, G. Ounoughene, C. R. Borra, K. Binnemans, and T. Van Gerven, “Neutralisation of bauxite residue by carbon dioxide prior to acidic leaching for metal recovery,” *Miner Eng*, vol. 112, no. July, pp. 92–102, 2017, https://doi.org/10.1016/j.mineng.2017.07.011.
[19] É. A. Deady, E. Mouchos, K. Goodenough, B. J. Williamson, and F. Wall, “A review of the potential for rare-earth element resources from European red muds: examples from Seydişehir, Turkey and Parnassus-Giona, Greece,” *Mineral Mag*, vol. 80, no. 1, pp. 43–61, 2016, https://doi.org/10.1180/minmag.2016.080.052.
[20] M. Ochsenkühn-Petropulu, Th. Lyberopulu, and G. Parissakis, “Direct determination of landthanides, yttrium and scandium in bauxites and red mud from alumina production,” *Anal Chim Acta*, vol. 296, no. 3, pp. 305–313, 1994, https://doi.org/10.1016/0003-2670(94)80250-5.
[21] C. Bonomi, C. Cardenia, P. T. W. Yin, and D. Panias, “Review of Technologies in the Recovery of Iron , Aluminium , Titanium and Rare Earth Elements from Bauxite Residue (Red Mud) Review of Technologies in the Recovery of Iron , Aluminium, Titanium and Rare Earth Elements from Bauxite Residue (Red Mud),” *3rd InternationalSymposium on Enhanced Landfill Mining | Lisbon – Portugal*, vol. 4, no. February 2016, pp. 259–276, 2016.
[22] E. Balomenos, I. Gianopoulou, D. Panias, and I. Paspaliaris, “ENEXAL: Novel technologies for enhanced energy and exergy efficiencies in primary aluminium production industry,” *Metalurgija – Journal of Metallurgy*, vol. 15, no. 4, pp. 203–217, 2009.
[23] P. Tam, W. Yin, B. Xakalashe, B. Friedrich, and D. Panias, “Carbothermic Reduction of Bauxite Residue for Iron Recovery and Subsequent Aluminium Recovery from Slag Leaching,” *35th International ICSOBA Conference, Hamburg, Germany, 2 – 5 October, 2017*, pp. 603–614, 2017.
[24] O. Ruiz, C. Clemente, M. Alonso, and F. J. Alguacil, “Recycling of an electric arc furnace flue dust to obtain high grade ZnO,” *J Hazard Mater*, vol. 141, no. 1, pp. 33–36, 2007, https://doi.org/10.1016/j.jhazmat.2006.06.079.
[25] J. A. de Araújo and V. Schalch, “Recycling of electric arc furnace (EAF) dust for use in steel making process,” *Journal of Materials Research and Technology*, vol. 3, no. 3, pp. 274–279, 2014, https://doi.org/10.1016/j.jmrt.2014.06.003.
[26] C. Cardenia, B. Xakalashe, E. Balomenos, and D. Panias, “Reductive Roasting Process for the Recovery of Iron Oxides from Bauxite Residue through Rotary Kiln Furnace and Magnetic Separation,” *35th International ICSOBA Conference, Hamburg, Germany, 2–5 October, 2017*, pp. 595–602, 2017.

[27] C. Bonomi, P. Davris, E. Balomenos, and I. Giannopoulou, “Ionometallurgical Leaching Process of Bauxite Residue : a Comparison between Hydrophilic and Hydrophobic Ionic Liquids,” *35th International ICSOBA Conference, Hamburg, Germany, 2–5 October, 2017*, pp. 557–564, 2017.
[28] A. Marmier, *Decarbonisation options for the cement industry*. Publications Office of the European Union, 2023. https://data.europa.eu/doi/10.2760/174037.
[29] P. E. Tsakiridis, S. Agatzini-Leonardou, and P. Oustadakis, “Red mud addition in the raw meal for the production of Portland cement clinker,” *J Hazard Mater*, vol. 116, no. 1–2, pp. 103–110, 2004, https://doi.org/10.1016/j.jhazmat.2004.08.002.
[30] International Aluminium Institute, “Opportunities for using bauxite residue in Portland Cement clinker production,” Mar. 2020. Accessed: May 20, 2025. [Online]. Available: https://international-aluminium.org/wp-content/uploads/2024/03/opportunities_for_use_of_bauxite_residue_in_portl.pdf
[31] J. L. Provis, A. Palomo, and C. Shi, “Advances in understanding alkali-activated materials,” *Cem Concr Res*, vol. 78, pp. 110–125, 2015, https://doi.org/10.1016/j.cemconres.2015.04.013.
[32] “ISO 14044:2006 Environmental management – Life cycle assessment – Requirements and guidelines,” Jul. 2006. Accessed: Nov. 21, 2025. [Online]. Available: https://www.iso.org/standard/38498.html
[33] “ISO 14040:2006 Environmental management – Life cycle assessment – Principles and framework,” Jul. 2006, *International Standard Organization*. Accessed: Nov. 21, 2025. [Online]. Available: https://www.iso.org/standard/37456.html
[34] JRC European commission, *ILCD Handbook: Recommendations for Life Cycle Impact Assessment in the European context*. Luxembourg: European Comission, 2011. https://doi.org/10.278/33030.
[35] European Commission, *Joint Research Centre – Institute for Environment and Sustainability: International Reference Life Cycle Data System (ILCD) Handbook-Recommendations for Life Cycle Impact Assessment in the European context.*, First edit. Luxembourg: Publications Office of the European Union, 2011. https://doi.org/10.278/33030.
[36] A. Meijer, M. Huijbregts, and L. Reijnders, “Human Health Damages due to Indoor Sources of Organic Compounds and Radioactivity in Life Cycle Impact Assessment of Dwellings – Part 1: Characterisation Factors (8 pp),” *Int J Life Cycle Assess*, vol. 10, no. 5, pp. 309–316, 2005, http://dx.doi.org/10.1065/lca2004.12.194.1.
[37] A. Meijer, M. Huijbregts, and L. Reijnders, “Human Health Damages due to Indoor Sources of Organic Compounds and Radioactivity in Life Cycle Impact Assessment of Dwellings – Part 2: Damage Scores (10 pp),” *Int J Life Cycle Assess*, vol. 10, no. 6, pp. 383–392, 2005, http://dx.doi.org/10.1065/lca2004.12.194.2.
[38] R. Frischknecht, A. Braunschweig, P. Hofstetter, and P. Suter, “Human health damages due to ionising radiation in life cycle impact assessment,” *Environ Impact Assess Rev*, vol. 20, no. 2, pp. 159–189, 2000, https://doi.org/10.1016/S0195-9255(99)00042-6.
[39] J. Garnier-Laplace, K. Beaugelin-Seiller, R. Gilbin, C. Della-Vedova, O. Jolliet, and J. Payet, “A Screening Level Ecological Risk Assessment and ranking method for liquid radioactive and chemical mixtures released by nuclear facilities under normal operating conditions,” *Radioprotection*, vol. 44, no. 5, pp. 903–908, 2009, https://doi.org/10.1051/radiopro/20095161.

[40] M. Z. Hauschild *et al.*, “Identifying best existing practice for characterization modeling in life cycle impact assessment,” *International Journal of Life Cycle Assessment*, vol. 18, no. 3, pp. 683–697, 2013, https://doi.org/10.1007/s11367-012-0489-5.
[41] IAEA, “Analytical Methodology for the Determination of Radium Isotopes in Environmental Samples,” no. IAEA/AQ/19, 2010.
[42] T. Vidmar, “EFFTRAN—A Monte Carlo efficiency transfer code for gamma-ray spectrometry,” *Nucl Instrum Methods Phys Res A*, vol. 550, no. 3, pp. 603–608, 2005, https://doi.org/10.1016/j.nima.2005.05.055.
[43] IAEA, “Preparation and certification of IAEA gamma-ray spectrometry reference materials RGU-1, RGTh-1 and RGK-1,” *Iaea-Rl-148*, no. August, p. 48, 1987.
[44] S. Suursoo, M. Kiisk, A. Semakalu, and K. Isakar, “Radon leakage as a source of additional uncertainty in simultaneous determination of 226Ra and 228Ra by gamma spectrometry—Validation of analysis procedure,” *Applied Radiation and Isotopes*, vol. 87, pp. 447–451, 2014, https://doi.org/10.1016/j.apradiso.2013.11.031.
[45] M. Markkanen, “Radiation Dose Assessments for Materials with Elevated Natural Radioactivity,” Helsinki, Nov. 1995.
[46] R. K. Rosenbaum *et al.*, “USEtox – The UNEP-SETAC toxicity model: Recommended characterisation factors for human toxicity and freshwater ecotoxicity in life cycle impact assessment,” *International Journal of Life Cycle Assessment*, vol. 13, no. 7, pp. 532–546, 2008, https://doi.org/10.1007/s11367-008-0038-4.
[47] M. Bijster *et al.*, “USEtox 2.0 Documentation (v2),” 2015. https://doi.org/10.11581/DTU:0000001.
[48] UNSCEAR, “Exposures from natural radiation sources,” pp. 84–141, 2000.
[49] K. F. Eckerman and J. C. Ryman, “Federal Guidance Report No. 12: External Exposure to Radionuclides in Air, Water, and Soil,” 1987.
[50] C. J. L. Murray, “Global burden of disease Quantifying the burden of disease: the technical basis for disability-adjusted life years,” *Bull World Health Organ*, vol. 72 (3), pp. 429–445, 1994.
[51] C. J. L. Murray, A. D. Lopez, and & D. T. Jamison3, “The global burden of disease in 1990: summary results, sensitivity analysis and future directions,” *Bull World Health Organ*, vol. 72 (3), pp. 495–509, 1994.
[52] D. W. Pennington, J. Payet, and M. Hauschild, “Aquatic ecotoxicological indicators in life-cycle assessment,” *Environ Toxicol Chem*, vol. 23, no. 7, pp. 1796–1807, Jul. 2004, https://doi.org/10.1897/03-157.
[53] J. E. Brown *et al.*, “The ERICA Tool,” *J Environ Radioact*, vol. 99, no. 9, pp. 1371–1383, 2008, https://doi.org/10.1016/j.jenvrad.2008.01.008.
[54] N. Beresford *et al.*, “D-ERICA: An integrated approach to the assessment and management of environmental risks from ionising radiation. Description of purpose, methodology and application,” 2007.
[55] D. Copplestone, J. Hingston, and A. Real, “The development and purpose of the FREDERICA radiation effects database,” *J Environ Radioact*, vol. 99, no. 9, pp. 1456–1463, 2008, https://doi.org/10.1016/j.jenvrad.2008.01.006.
[56] Ecoinvent, “Cement, portland, Europe without Switzerland, Allocation, default, ecoinvent database version 3.2,” Nov. 2015. Accessed: May 20, 2025. [Online]. Available: https://support.ecoinvent.org/ecoinvent-version-3.2
[57] E. L. Barrera, E. Rosa, H. Spanjers, O. Romero, S. De Meester, and J. Dewulf, “A comparative assessment of anaerobic digestion power plants as alternative to lagoons for vinasse treatment: life cycle assessment and exergy analysis,” *J Clean Prod*, vol. 113, pp. 459–471, 2016, https://doi.org/10.1016/j.jclepro.2015.11.095.

[58] T. Vandermeersch, R. A. F. Alvarenga, P. Ragaert, and J. Dewulf, “Environmental sustainability assessment of food waste valorization options,” *Resour Conserv Recycl*, vol. 87, pp. 57–64, 2014, https://doi.org/10.1016/j.resconrec.2014.03.008.
[59] G. Wernet, C. Bauer, B. Steubing, J. Reinhard, E. Moreno-Ruiz, and B. Weidema, “The ecoinvent database version 3 (part I): overview and methodology,” *International Journal of Life Cycle Assessment*, vol. 21, pp. 1218–1230, 2016, https://doi.org/10.1007/s11367-016-1087-8.
[60] B. P. Weidema *et al.*, “The ecoinvent database: Overview and methodology, Data quality guideline for the ecoinvent database version 3, www.ecoinvent.org,” St. Gallen, May 2013. Accessed: May 20, 2025. [Online]. Available: https://vbn.aau.dk/ws/portalfiles/portal/176769045/Overview_and_methodology.pdf
[61] Y. Pontikes, “Utilization of red mud in the heavy clay industry,” PhD thesis, University of Patras, Patras, 2007.
[62] I. Vangelatos, G. N. Angelopoulos, and D. Boufounos, “Utilization of ferroalumina as raw material in the production of Ordinary Portland Cement,” *J Hazard Mater*, vol. 168, no. 1, pp. 473–478, 2009, https://doi.org/10.1016/j.jhazmat.2009.02.049.
[63] R. Trevisi, S. Risica, M. D’Alessandro, D. Paradiso, and C. Nuccetelli, “Natural radioactivity in building materials in the European Union: A database and an estimate of radiological significance,” *J Environ Radioact*, vol. 105, pp. 11–20, 2012, https://doi.org/10.1016/j.jenvrad.2011.10.001.
[64] P. Bossew, “The radon emanation power of building materials, soils and rocks,” *Applied Radiation and Isotopes*, vol. 59, no. 5–6, pp. 389–392, 2003, https://doi.org/10.1016/j.apradiso.2003.07.001.
[65] W. W. Nazaroff and A. V. Jr. Nero, *Radon and its decay products in indoor air*. John Wiley and Sons, Incorporated., 1988.
[66] Ecoinvent, “ecoinvent database Version 3.3.” Accessed: May 20, 2025. [Online]. Available: https://support.ecoinvent.org/ecoinvent-version-3.3
[67] A. Goronovski, P. J. Joyce, A. Björklund, G. Finnveden, and A. H. Tkaczyk, “Impact assessment of enhanced exposure from Naturally Occurring Radioactive Materials (NORM) within LCA,” *J Clean Prod*, 2017, http://doi.org/10.1016/j.jclepro.2017.11.131.
[68] “Characterisation factors of the ILCD Recommended Life Cycle Impact Assessment methods. Database and Supporting Information. First edition,” Luxembourg, Feb. 2012. https://doi.org/10.2788/60825.
[69] C. Sato, S. Kazama, A. Sakamoto, and K. Hirayanagi, “Behavior of Radioactive Elements (Uranium and Thorium) in Bayer Process,” in *Essential Readings in Light Metals*, John Wiley & Sons, Ltd, 2013, pp. 191–197. https://doi.org/10.1002/9781118647868.ch25.
[70] J. A. S. Adams and K. A. Richardson, “Radioactivity of aluminum metal,” *Economic Geology*, vol. 55, no. 5, pp. 1060–1063, Aug. 1960, https://doi.org/10.2113/gsecongeo.55.5.1060.
[71] I. Siotis and A. D. Wrixon, “Radiological consequences of the use of fly ash in building materials in Greece,” *Radiat Prot Dosimetry*, vol. 7, no. 1–4, pp. 101–105, 1984, https://doi.org/10.1093/oxfordjournals.rpd.a082972.
[72] D. Ariño-Montoya, R. I. Iacobescu, G. Giannakopoulos, M. S. Katsiotis, and Y. Pontikes, “From bauxite residue to calcium sulfo-ferroaluminate cement: Study of the clinkerization and hydration kynetics,” in *12ο Πανελλήνιο Επιστημονικό Συνέδριο Χημικής Μηχανικής*, Athens, May 2019. [Online]. Available: https://www.researchgate.net/publication/333395137

ACKNOWLEDGEMENTS

This thesis is the culmination of my research work at the University of Tartu. This was a rough journey with ups and downs, and I am deeply grateful to those who have shared this path with me.

First, I would like to express my gratitude to my colleagues at the University of Tartu, Madis Kiisk, Siiri Salupere, Taavi Vaasma, Rein Koch, Maria Leier, Kaisa Putk and my supervisor Alan Henry Tkaczyk. Thank you for your time and effort spent with me and for making my stay at the university of Tartu enjoyable.

I extend my sencere gratitude to the ETN REDMUD team: all the team reaserchers that made my scientific journey joyful, their supervisors and the team coordinators that made this project possible and opened the world of chemistry and metallurgy for me. I am wholeheartedly thankful to Anna Björklund, Vicky Vassiliadou, Dimitrios Panias and Marios Katsiotis for hosting me at their instutions during my research secondments and to Peter James Joyce, Johannes Vind, Pritii Tam Wai Yin, Rodolfo Marin Rivera and David Ariño Montoya for making this time a memorable experience.

I am deeply pleased to thank Nathalie Vanhoudt research group at the SCK-CEN research institution and members of the NORM4Building network who have willingly shared their knowledge and experience. Special thanks to Jordi Vives i Batlle for his optimism and faith in me.

The research leading to these results has received funding from the European Union's Horizon 2020 research and innovation programme (H2020/2014–2019) under Grant Agreement No. 636876 (MSCA-ETN REDMUD). This publication reflects only the authors' view, exempting the European Union from any liability. Project website: http://www.etn.redmud.org. The author would like to acknowledge the support of an STSM Grant from COST Action TU1301 NORM4Building, supported by the COST Association (European Cooperation in Science and Technology).

Finally, thank you to my friends, family and my current colleagues at Fermi Energia for your endless source of motivation and trust in me. Without your warmest support and never-ending trust in me this milestone of my life would not be achieved.

PUBLICATIONS

CURRICULUM VITAE

Name: Andrei Goronovski
Date of birth: 07.07.1988
Citizenship: Estonian
Gender: Male
Email: goronovski@gmail.com

Education

2015–2026	University of Tartu, PhD in Physics
2011–2012	Royal Institute of Technology, MSc in Nuclear Energy Engineering
2008–2010	Tallinn University of Technology, BSc in Electrical Engineering

Languages

Russian, Ukrainian, Estonian, English

Professional employment

2022–…	Fermi Energia; Nuclear Engineer
2020–2022	ABB; R&D Mechanical Engineer
2015–2020	University of Tartu, Institute of Physics; Junior Research Fellow in Physics
2012–2015	Royal Institute of Technology, Research Engineer

Research interests

Public and environment protection from ionizing radiation; NORM; nuclear power safety

Publications

P. J. Joyce, **A. Goronovski**, A. H. Tkaczyk, and A. Björklund, "A framework for including enhanced exposure to naturally occurring radioactive materials (NORM) in LCA," *Int. J. Life Cycle Assess.*, vol. 22, no. 7, 2017. https://doi.org/10.1007/s11367-016-1218-2

A. Goronovski, P. J. Joyce, A. Björklund, G. Finnveden, and A. H. Tkaczyk, "Impact assessment of enhanced exposure from Naturally Occurring Radioactive Materials (NORM) within LCA," *J. Clean. Prod.*, 2017. https://doi.org/10.1016/j.jclepro.2017.11.131

P. J. Joyce, T. Hertel, **A. Goronovski**, A. H. Tkaczyk, Y. Pontikes, and A. Björklund, "Identifying hotspots of environmental impact in the development of novel inorganic polymer paving blocks from bauxite residue," *Resour. Conserv. Recycl.*, vol. 138, no. April, pp. 87–98, 2018. https://doi.org/10.1016/j.resconrec.2018.07.006

A. Goronovski, J. Vind, V. Vassiliadou, D. Panias, and A. H. Tkaczyk, "Radiological assessment of the Bayer process," *Miner. Eng.*, vol. 137, no. April, pp. 250–258, 2019. https://doi.org/10.1016/j.mineng.2019.04.016

A. Goronovski and A. H. Tkaczyk, "Radiological assessment of the bauxite residue valorization chain," *J. Radioanal. Nucl. Chem.*, vol. 321, no. 3, pp. 955–963, 2019. http://doi.org/10.1007/s10967-019-06676-6

A. Goronovski, R. M. Rivera, T. Van Gerven, and A. H. Tkaczyk, "Radiological assessment of bauxite residue processing to enable zero-waste valorisation and regulatory compliance," *J. Clean. Prod.*, vol. 294, p. 125165, 2021. http://dx.doi.org/10.1016/j.jclepro.2020.125165

ELULOOKIRJELDUS

Nimi: Andrei Goronovski
Sünniaeg: 07.07.1988
Kodakondsus: Eesti
Sugu: Mees
Email: goronovski@gmail.com

Haridus

2015–2026	Tartu Ülikool, Füüsika õppekava, PhD
2011–2012	Royal Institute of Technology (KTH), Tuuma Energeetika Insener, MSc
2008–2010	Tallinna Tehnikaülikool, Elektroenergeetika, BSc

Keelteoskus

Vene, Ukraina, Eesti, Inglise

Töökogemus

2022–…	Fermi Energia; Tuumaenergia Insener
2020–2022	ABB; R&D Mehaanika Insener
2015–2020	Tartu Ülikool, Füüsika Instituut; Füüsika Nooremteadur
2012–2015	Royal Institute of Technology (KTH), Arendus Insener

Teadustöö põhisuunad

Avalikkuse ja keskkonna kaitse ioniseeriva kiirguse eest; NORM; tuumaenergia ohutus

Publikatsioonid

P. J. Joyce, **A. Goronovski**, A. H. Tkaczyk, and A. Björklund, "A framework for including enhanced exposure to naturally occurring radioactive materials (NORM) in LCA," *Int. J. Life Cycle Assess.*, vol. 22, no. 7, 2017. https://doi.org/10.1007/s11367-016-1218-2

A. Goronovski, P. J. Joyce, A. Björklund, G. Finnveden, and A. H. Tkaczyk, "Impact assessment of enhanced exposure from Naturally Occurring Radioactive Materials (NORM) within LCA," *J. Clean. Prod.*, 2017. https://doi.org/10.1016/j.jclepro.2017.11.131

P. J. Joyce, T. Hertel, **A. Goronovski**, A. H. Tkaczyk, Y. Pontikes, and A. Björklund, "Identifying hotspots of environmental impact in the development of novel inorganic polymer paving blocks from bauxite residue," *Resour. Conserv. Recycl.*, vol. 138, no. April, pp. 87–98, 2018. https://doi.org/10.1016/j.resconrec.2018.07.006

A. Goronovski, J. Vind, V. Vassiliadou, D. Panias, and A. H. Tkaczyk, "Radiological assessment of the Bayer process," *Miner. Eng.*, vol. 137, no. April, pp. 250–258, 2019. https://doi.org/10.1016/j.mineng.2019.04.016

A. Goronovski and A. H. Tkaczyk, "Radiological assessment of the bauxite residue valorization chain," *J. Radioanal. Nucl. Chem.*, vol. 321, no. 3, pp. 955–963, 2019. http://doi.org/10.1007/s10967-019-06676-6

A. Goronovski, R. M. Rivera, T. Van Gerven, and A. H. Tkaczyk, "Radiological assessment of bauxite residue processing to enable zero-waste valorisation and regulatory compliance," *J. Clean. Prod.*, vol. 294, p. 125165, 2021. http://dx.doi.org/10.1016/j.jclepro.2020.125165

DISSERTATIONES PHYSICAE UNIVERSITATIS TARTUENSIS

1. **Andrus Ausmees**. XUV-induced electron emission and electron-phonon interaction in alkali halides. Tartu, 1991.
2. **Heiki Sõnajalg**. Shaping and recalling of light pulses by optical elements based on spectral hole burning. Tartu, 1991.
3. **Sergei Savihhin**. Ultrafast dynamics of F-centers and bound excitons from picosecond spectroscopy data. Tartu, 1991.
4. **Ergo Nõmmiste**. Leelishalogeniidide röntgenelektronemissioon kiiritamisel footonitega energiaga 70–140 eV. Tartu, 1991.
5. **Margus Rätsep**. Spectral gratings and their relaxation in some low-temperature impurity-doped glasses and crystals. Tartu, 1991.
6. **Tõnu Pullerits**. Primary energy transfer in photosynthesis. Model calculations. Tartu, 1991.
7. **Olev Saks**. Attoampri diapasoonis voolude mõõtmise füüsikalised alused. Tartu, 1991.
8. **Andres Virro**. AlGaAsSb/GaSb heterostructure injection lasers. Tartu, 1991.
9. **Hans Korge**. Investigation of negative point discharge in pure nitrogen at atmospheric pressure. Tartu, 1992.
10. **Jüri Maksimov**. Nonlinear generation of laser VUV radiation for high-resolution spectroscopy. Tartu, 1992.
11. **Mark Aizengendler**. Photostimulated transformation of aggregate defects and spectral hole burning in a neutron-irradiated sapphire. Tartu, 1992.
12. **Hele Siimon**. Atomic layer molecular beam epitaxy of A^2B^6 compounds described on the basis of kinetic equations model. Tartu, 1992.
13. **Tõnu Reinot**. The kinetics of polariton luminescence, energy transfer and relaxation in anthracene. Tartu, 1992.
14. **Toomas Rõõm**. Paramagnetic H^{2-} and F^+ centers in CaO crystals: spectra, relaxation and recombination luminescence. Tallinn, 1993.
15. **Erko Jalviste**. Laser spectroscopy of some jet-cooled organic molecules. Tartu, 1993.
16. **Alvo Aabloo**. Studies of crystalline celluloses using potential energy calculations. Tartu, 1994.
17. **Peeter Paris**. Initiation of corona pulses. Tartu, 1994.
18. **Павел Рубин**. Локальные дефектные состояния в CuO_2 плоскостях высокотемпературных сверхпроводников. Тарту, 1994.
19. **Olavi Ollikainen**. Applications of persistent spectral hole burning in ultrafast optical neural networks, time-resolved spectroscopy and holographic interferometry. Tartu, 1996.
20. **Ülo Mets**. Methodological aspects of fluorescence correlation spectroscopy. Tartu, 1996.
21. **Mikhail Danilkin**. Interaction of intrinsic and impurity defects in CaS:Eu luminophors. Tartu, 1997.

22. **Ирина Кудрявцева**. Создание и стабилизация дефектов в кристаллах KBr, KCl, RbCl при облучении ВУФ-радиацией. Тарту, 1997.
23. **Andres Osvet**. Photochromic properties of radiation-induced defects in diamond. Tartu, 1998.
24. **Jüri Örd**. Classical and quantum aspects of geodesic multiplication. Tartu, 1998.
25. **Priit Sarv**. High resolution solid-state NMR studies of zeolites. Tartu, 1998.
26. **Сергей Долгов**. Электронные возбуждения и дефектообразование в некоторых оксидах металлов. Тарту, 1998.
27. **Kaupo Kukli**. Atomic layer deposition of artificially structured dielectric materials. Tartu, 1999.
28. **Ivo Heinmaa**. Nuclear resonance studies of local structure in $RBa_2Cu_3O_{6+x}$ compounds. Tartu, 1999.
29. **Aleksander Shelkan**. Hole states in CuO_2 planes of high temperature superconducting materials. Tartu, 1999.
30. **Dmitri Nevedrov**. Nonlinear effects in quantum lattices. Tartu, 1999.
31. **Rein Ruus**. Collapse of 3d (4f) orbitals in 2p (3d) excited configurations and its effect on the x-ray and electron spectra. Tartu, 1999.
32. **Valter Zazubovich**. Local relaxation in incommensurate and glassy solids studied by Spectral Hole Burning. Tartu, 1999.
33. **Indrek Reimand**. Picosecond dynamics of optical excitations in GaAs and other excitonic systems. Tartu, 2000.
34. **Vladimir Babin**. Spectroscopy of exciton states in some halide macro- and nanocrystals. Tartu, 2001.
35. **Toomas Plank**. Positive corona at combined DC and AC voltage. Tartu, 2001.
36. **Kristjan Leiger**. Pressure-induced effects in inhomogeneous spectra of doped solids. Tartu, 2002.
37. **Helle Kaasik**. Nonperturbative theory of multiphonon vibrational relaxation and nonradiative transitions. Tartu, 2002.
38. **Tõnu Laas**. Propagation of waves in curved spacetimes. Tartu, 2002.
39. **Rünno Lõhmus**. Application of novel hybrid methods in SPM studies of nanostructural materials. Tartu, 2002.
40. **Kaido Reivelt**. Optical implementation of propagation-invariant pulsed free-space wave fields. Tartu, 2003.
41. **Heiki Kasemägi**. The effect of nanoparticle additives on lithium-ion mobility in a polymer electrolyte. Tartu, 2003.
42. **Villu Repän**. Low current mode of negative corona. Tartu, 2004.
43. **Алексей Котлов**. Оксианионные диэлектрические кристаллы: зонная структура и электронные возбуждения. Tartu, 2004.
44. **Jaak Talts**. Continuous non-invasive blood pressure measurement: comparative and methodological studies of the differential servo-oscillometric method. Tartu, 2004.
45. **Margus Saal**. Studies of pre-big bang and braneworld cosmology. Tartu, 2004.

46. **Eduard Gerškevitš**. Dose to bone marrow and leukaemia risk in external beam radiotherapy of prostate cancer. Tartu, 2005.
47. **Sergey Shchemelyov**. Sum-frequency generation and multiphoton ionization in xenon under excitation by conical laser beams. Tartu, 2006.
48. **Valter Kiisk**. Optical investigation of metal-oxide thin films. Tartu, 2006.
49. **Jaan Aarik**. Atomic layer deposition of titanium, zirconium and hafnium dioxides: growth mechanisms and properties of thin films. Tartu, 2007.
50. **Astrid Rekker**. Colored-noise-controlled anomalous transport and phase transitions in complex systems. Tartu, 2007.
51. **Andres Punning**. Electromechanical characterization of ionic polymer-metal composite sensing actuators. Tartu, 2007.
52. **Indrek Jõgi**. Conduction mechanisms in thin atomic layer deposited films containing TiO_2. Tartu, 2007.
53. **Aleksei Krasnikov**. Luminescence and defects creation processes in lead tungstate crystals. Tartu, 2007.
54. **Küllike Rägo**. Superconducting properties of MgB_2 in a scenario with intra- and interband pairing channels. Tartu, 2008.
55. **Els Heinsalu**. Normal and anomalously slow diffusion under external fields. Tartu, 2008.
56. **Kuno Kooser**. Soft x-ray induced radiative and nonradiative core-hole decay processes in thin films and solids. Tartu, 2008.
57. **Vadim Boltrushko**. Theory of vibronic transitions with strong nonlinear vibronic interaction in solids. Tartu, 2008.
58. **Andi Hektor**. Neutrino Physics beyond the Standard Model. Tartu, 2008.
59. **Raavo Josepson**. Photoinduced field-assisted electron emission into gases. Tartu, 2008.
60. **Martti Pärs**. Study of spontaneous and photoinduced processes in molecular solids using high-resolution optical spectroscopy. Tartu, 2008.
61. **Kristjan Kannike**. Implications of neutrino masses. Tartu, 2008.
62. **Vigen Issahhanjan**. Hole and interstitial centres in radiation-resistant MgO single crystals. Tartu, 2008.
63. **Veera Krasnenko**. Computational modeling of fluorescent proteins. Tartu, 2008.
64. **Mait Müntel**. Detection of doubly charged higgs boson in the CMS detector. Tartu, 2008.
65. **Kalle Kepler**. Optimisation of patient doses and image quality in diagnostic radiology. Tartu, 2009.
66. **Jüri Raud**. Study of negative glow and positive column regions of capillary HF discharge. Tartu, 2009.
67. **Sven Lange**. Spectroscopic and phase-stabilisation properties of pure and rare-earth ions activated ZrO_2 and HfO_2. Tartu, 2010.
68. **Aarne Kasikov**. Optical characterization of inhomogeneous thin films. Tartu, 2010.
69. **Heli Valtna-Lukner**. Superluminally propagating localized optical pulses. Tartu, 2010.

70. **Artjom Vargunin**. Stochastic and deterministic features of ordering in the systems with a phase transition. Tartu, 2010.
71. **Hannes Liivat**. Probing new physics in e+e− annihilations into heavy particles via spin orientation effects. Tartu, 2010.
72. **Tanel Mullari**. On the second order relativistic deviation equation and its applications. Tartu, 2010.
73. **Aleksandr Lissovski**. Pulsed high-pressure discharge in argon: spectroscopic diagnostics, modeling and development. Tartu, 2010.
74. **Aile Tamm**. Atomic layer deposition of high-permittivity insulators from cyclopentadienyl-based precursors. Tartu, 2010.
75. **Janek Uin**. Electrical separation for generating standard aerosols in a wide particle size range. Tartu, 2011.
76. **Svetlana Ganina**. Hajusandmetega ülesanded kui üks võimalus füüsikaõppe efektiivsuse tõstmiseks. Tartu, 2011
77. **Joel Kuusk**. Measurement of top-of-canopy spectral reflectance of forests for developing vegetation radiative transfer models. Tartu, 2011.
78. **Raul Rammula**. Atomic layer deposition of HfO_2 – nucleation, growth and structure development of thin films. Tartu, 2011.
79. **Сергей Наконечный**. Исследование электронно-дырочных и интерстициал-вакансионных процессов в монокристаллах MgO и LiF методами термоактивационной спектроскопии. Тарту, 2011.
80. **Niina Voropajeva**. Elementary excitations near the boundary of a strongly correlated crystal. Tartu, 2011.
81. **Martin Timusk**. Development and characterization of hybrid electro-optical materials. Tartu, 2012, 106 p.
82. **Merle Lust**. Assessment of dose components to Estonian population. Tartu, 2012, 84 p.
83. **Karl Kruusamäe**. Deformation-dependent electrode impedance of ionic electromechanically active polymers. Tartu, 2012, 128 p.
84. **Liis Rebane**. Measurement of the $W \to \tau\nu$ cross section and a search for a doubly charged Higgs boson decaying to τ-leptons with the CMS detector. Tartu, 2012, 156 p.
85. **Jevgeni Šablonin**. Processes of structural defect creation in pure and doped MgO and NaCl single crystals under condition of low or super high density of electronic excitations. Tartu, 2013, 145 p.
86. **Riho Vendt**. Combined method for establishment and dissemination of the international temperature scale. Tartu, 2013, 108 p.
87. **Peeter Piksarv**. Spatiotemporal characterization of diffractive and non-diffractive light pulses. Tartu, 2013, 156 p.
88. **Anna Šugai**. Creation of structural defects under superhigh-dense irradiation of wide-gap metal oxides. Tartu, 2013, 108 p.
89. **Ivar Kuusik**. Soft X-ray spectroscopy of insulators. Tartu, 2013, 113 p.
90. **Viktor Vabson**. Measurement uncertainty in Estonian Standard Laboratory for Mass. Tartu, 2013, 134 p.

91. **Kaupo Voormansik**. X-band synthetic aperture radar applications for environmental monitoring. Tartu, 2014, 117 p.
92. **Deivid Pugal**. hp-FEM model of IPMC deformation. Tartu, 2014, 143 p.
93. **Siim Pikker**. Modification in the emission and spectral shape of photo-stable fluorophores by nanometallic structures. Tartu, 2014, 98 p.
94. **Mihkel Pajusalu**. Localized Photosynthetic Excitons. Tartu, 2014, 183 p.
95. **Taavi Vaikjärv**. Consideration of non-adiabaticity of the Pseudo-Jahn-Teller effect: contribution of phonons. Tartu, 2014, 129 p.
96. **Martin Vilbaste**. Uncertainty sources and analysis methods in realizing SI units of air humidity in Estonia. Tartu, 2014, 111 p.
97. **Mihkel Rähn**. Experimental nanophotonics: single-photon sources- and nanofiber-related studies. Tartu, 2015, 107 p.
98. **Raul Laasner**. Excited state dynamics under high excitation densities in tungstates. Tartu, 2015, 125 p.
99. **Andris Slavinskis**. EST Cube-1 attitude determination. Tartu, 2015, 104 p.
100. **Karlis Zalite**. Radar Remote Sensing for Monitoring Forest Floods and Agricultural Grasslands. Tartu, 2016, 124 p.
101. **Kaarel Piip**. Development of LIBS for *in-situ* study of ITER relevant materials. Tartu, 2016, 93 p.
102. **Kadri Isakar**. ^{210}Pb in Estonian air: long term study of activity concentrations and origin of radioactive lead. Tartu, 2016, 107 p.
103. **Artur Tamm**. High entropy alloys: study of structural properties and irradiation response. Tartu, 2016, 115 p.
104. **Rasmus Talviste**. Atmospheric-pressure He plasma jet: effect of dielectric tube diameter. Tartu, 2016, 107 p.
105. **Andres Tiko**. Measurement of single top quark properties with the CMS detector. Tartu, 2016, 161 p.
106. **Aire Olesk**. Hemiboreal Forest Mapping with Interferometric Synthetic Aperture Radar. Tartu, 2016, 121 p.
107. **Fred Valk**. Nitrogen emission spectrum as a measure of electric field strength in low-temperature gas discharges. Tartu, 2016, 149 p.
108. **Manoop Chenchiliyan**. Nano-structural Constraints for the Picosecond Excitation Energy Migration and Trapping in Photosynthetic Membranes of Bacteria. Tartu, 2016, 115p.
109. **Lauri Kaldamäe**. Fermion mass and spin polarisation effects in top quark pair production and the decay of the higgs boson. Tartu, 2017, 104 p.
110. **Marek Oja**. Investigation of nano-size α- and transition alumina by means of VUV and cathodoluminescence spectroscopy. Tartu, 2017, 89 p.
111. **Viktoriia Levushkina**. Energy transfer processes in the solid solutions of complex oxides. Tartu, 2017, 101 p.
112. **Mikk Antsov**. Tribomechanical properties of individual 1D nanostructures: experimental measurements supported by finite element method simulations. Tartu, 2017, 101 p.
113. **Hardi Veermäe**. Dark matter with long range vector-mediated interactions. Tartu, 2017, 137 p.

114. **Aris Auzans**. Development of computational model for nuclear energy systems analysis: natural resources optimisation and radiological impact minimization. Tartu, 2018, 138 p.
115. **Aleksandr Gurev**. Coherent fluctuating nephelometry application in laboratory practice. Tartu, 2018, 150 p.
116. **Ardi Loot**. Enhanced spontaneous parametric downconversion in plasmonic and dielectric structures. Tartu, 2018, 164 p.
117. **Andreas Valdmann**. Generation and characterization of accelerating light pulses. Tartu, 2019, 85 p.
118. **Mikk Vahtrus**. Structure-dependent mechanical properties of individual one-dimensional metal-oxide nanostructures. Tartu, 2019, 110 p.
119. **Ott Vilson**. Transformation properties and invariants in scalar-tensor theories of gravity. Tartu, 2019, 183 p.
120. **Indrek Sünter**. Design and characterisation of subsystems and software for ESTCube-1 nanosatellite. Tartu, 2019, 195 p.
121. **Marko Eltermann**. Analysis of samarium doped TiO_2 optical and multiresponse oxygen sensing capabilities. Tartu, 2019, 113 p.
122. **Kalev Erme**. The effect of catalysts in plasma oxidation of nitrogen oxides. Tartu, 2019, 114 p.
123. **Sergey Koshkarev**. A phenomenological feasibility study of the possible impact of the intrinsic heavy quark (charm) mechanism on the production of doubly heavy mesons and baryons. Tartu, 2020, 134 p.
124. **Kristi Uudeberg**. Optical Water Type Guided Approach to Estimate Water Quality in Inland and Coastal Waters. Tartu, 2020, 222 p.
125. **Daniel Blixt**. Hamiltonian analysis of covariant teleparallel theories of gravity. Tartu, 2021, 142 p.
126. **Ulbossyn Ualikhanova**. Gravity theories based on torsion: theoretical and observational constraints. Tartu, 2021, 154 p.
127. **Iaroslav Iakubivskyi**. Nanospacecraft for Technology Demonstration and Science Missions. Tartu, 2021, 177 p.
128. **Heido Trofimov**. Polluted clouds at air pollution hot spots help to better understand anthropogenic impacts on Earth's climate. Tartu, 2022, 96 p.
129. **Ott Rebane**. *In situ* non-contact sensing of microbiological contamination by fluorescence spectroscopy. Tartu, 2022, 157 p.
130. **Juhan Saaring**. Ultrafast Relaxation Processes in Ternary Hexafluorides Studied under Synchrotron Radiation Excitation. Tartu, 2022, 106 p.
131. **Ahmet Ilker Topuz**. Quantitative and qualitative investigations for muon scattering tomography via GEANT4 simulations: A computational study. Tartu, 2023, 163 p.
132. **Nico Benincasa**. Phase transitions and gravitational waves in models of dark matter. Tartu, 2023, 206 p.
133. **Kaja Pae**. Electron-phonon interactions in local degenerate electronic states in solids. Tartu, 2024, 201 p.
134. **Kristjan Müürsepp**. Phenomenological implications of Standard Model extensions. Tartu, 2024, 136 p.

135. **Ye Wang**. Investigating the properties of metal surfaces under high electric fields based on ab initio calculations. Tartu, 2024, 107 p.
136. **Laxmipriya Pati**. The effects of non-Riemannian connection in teleparallel gravity. Tartu, 2025, 172 p.
137. **Débora Aguiar Gomes**. Theoretical and astrophysical aspects of extended general relativity. Tartu, 2025, 169 p.
138. **Mina Hajizadeh Omaslanolya**. Structure and dynamics of photoactive proteins studied by (in situ-) neutron scattering methods. Tartu, 2025, 150 p.
139. **Aditya Savio Paul**. Advancing the study of small solar system bodies through multi-agent mapping and characterization. Tartu, 2025, 244 p.
140. **Sanu Bifal Maji**. Synthesis and luminescence investigation of nano-particles doped with Pr^{3+} ions in selected fluoride and phosphate hosts. Tartu, 2025, 114 p.
141. **Ernest Michael Priidik Gallagher**. On the internal gauge theory analogy to the Cartan Khronon theory of gravity. Tartu, 2026, 221 p.
142. **Maria Naeem**. First order electroweak radiative corrections to the decay of the polarised *W* boson. Tartu, 2026, 236 p.
143. **Konstantinos Pallikaris**. Novel black holes in Einstein gravity. Tartu, 2026, 133 p.
144. **Aleksei Kubarski**. Dynamical symmetry breaking and dark matter. Tartu, 2026, 133 p.
145. **Lucy Zheng**. Cartan Khronon – Real space-time structure. Tartu, 2026, 193 p.
146. **Muhammad Usama Jamal**. Energy transfer to luminescence centres in alkali and rare-earth metal molybdates. Tartu, 2026, 100 p.
147. **Vasiliki Karanasou**. Exotic spherically symmetric objects in modified gravity. Tartu, 2026, 134 p.